

1 **Response to comments of reviewer 1 on**

2 **"Ice phase in Altocumulus Clouds over Leipzig: Remote sensing observa-**
3 **tions and detailed modelling" by Simmel et al.**

4 <http://www.atmos-chem-phys-discuss.net/15/1573/2015/>

5 We thank the reviewer for his/her constructive suggestions and for generally accepting
6 the paper when the proposed revisions are realised.

7 New text of the manuscript is cited in *italic*. Revised manuscript with highlighted
8 changes is given as supplement.

9 **Reviewer 1**

10 General coments

11 The authors study two altocumulus cloud case studies that were observed over Ger-
12 many via ground-based remote sensing. The cases were selected to represent the warmest
13 possible ice formation and more typically cold ice formation within altocumulus. The
14 authors apply an axisymmetric 1D model with spectral microphysics. The model is ini-
15 tialized with observed or model-derived thermodynamic profiles. Varying assumptions
16 are made regarding prescribed vertical motions, aerosol and ice nucleus properties, and
17 ice habit. Generally little work has been done on altocumulus microphysics, but that
18 which has been done requires more review in the introduction and conclusions to moti-
19 vate this work and to place the results into context. The approach is generally sound, but
20 not enough details are provided to allow the work to be reproduced. The observations
21 should be shown and described more completely. Overall, this work merits publication
22 after revisions to the manuscript that can readily address specific comments below.

23 Specific comments (page/line number if relevant)

24 1. The scientific questions to be addressed are not adequately stated. Ice nucleation
25 is discussed in the very short introduction, but no questions are targeted for this study.
26 This is perhaps related to the problem that the authors provide no background on
27 altocumulus. Has any study simulated such clouds before? Why did the authors choose
28 to use a model? Why this model with elaborate microphysics but simple dynamics? Has
29 any literature drawn conclusions about altocumulus relevant to this study? Does this
30 study produce conclusions that are consistent with past literature? References should
31 include Fleishauer et al. (JGR 59:1779, 2002), for instance.

32 **Authors**

33 Altocumulus clouds are a good example for shallow mixed-phase clouds with comparably
34 simple vertical structure — at least for the single-layered cases as they are considered
35 here. Therefore, a dynamically simple model setup with prescribed vertical velocity was
36 chosen to remain close to the observations. Feedback of microphysics on dynamics is
37 not considered to concentrate on primary microphysical effects and to avoid misleading
38 conclusions about secondary effects due to changed dynamics. A model intercomparison
39 study by Ovchinnikov et al. (2013, doi:10.1002/2013MS000282) has shown that bulk
40 microphysical models tend to underestimate ice growth by vapor deposition due to the
41 underlying ice distribution assumptions. In contrast to this, bin models directly simulate
42 the shape of the distributions and, therefore, no assumptions concerning the shape have
43 to be made.

44 The underlying topic is mixed-phase microphysics and the interaction between the
45 three phases of water. It is well-known that due to the different saturation pressure
46 of water vapor with respect to liquid water and ice, a mixed-phase cloud is in a non-
47 equilibrium state which, nevertheless, may lead to a quasi-steady existence (e.g., Korolev
48 and Field, 2008, JAS). To study those interactions, a bin model is suited well, since
49 condensational/depositional growth is not only described by saturation adjustment but
50 by a detailed description of sub-/supersaturation of each size bin resulting in different
51 growth rates. This automatically results in a very detailed description of the Wegener-
52 Bergeron-Findeisen (WBF) process which drives the phase interaction (see also response
53 to review 3).

54 *According to Warren et al. (1998a,b) altocumulus and altostratus clouds together cover*
55 *22 % of the earth's surface. For single-layered altocumulus clouds, ...*

56 *... This was previously reported from Fleishauer et al. (2002) and Carey et al. (2008).*
57 *Fleishauer et al. (2002) also emphasized a lack of significant temperature inversions or*
58 *wind shears as a major feature of these clouds. Kanitz et al. (2011) show that the ratio of*
59 *ice-containing clouds increases with decreasing temperature. However, the numbers are*
60 *different for different locations with similar dynamics but with different aerosol burden,*
61 *e.g., at northern and southern midlatitudes, underlining the question for the influence*
62 *of ice-nucleating particles (INP). ...*

63 *... However, despite its important contribution, ice nucleation does not determine*
64 *the entire microphysics of mixed-phase clouds alone. It is rather the complex trans-*
65 *fer between the three phases of water: water vapor, liquid water and ice described by*
66 *the Wegener-Bergeron-Findeisen (WBF) mechanism (Wegener, 1911; Bergeron, 1935;*
67 *Findeisen, 1938). It is well-known that due to the different saturation pressures of water*
68 *vapor with respect to liquid water and ice, a mixed-phase cloud is in a non-equilibrium*
69 *state which, nevertheless, may lead to a quasi-steady existence (Korolev and Field, 2008).*
70 *The main drivers for this phase transfer are vertical velocity (leading to supersaturation*
71 *and subsequent droplet formation) and ice particle formation and growth (WBF starts)*
72 *leading to sedimentation of the typically fast growing ice particles (WBF ends due to*
73 *removal of ice). The motivation of this work is to shed more light on the relative contri-*

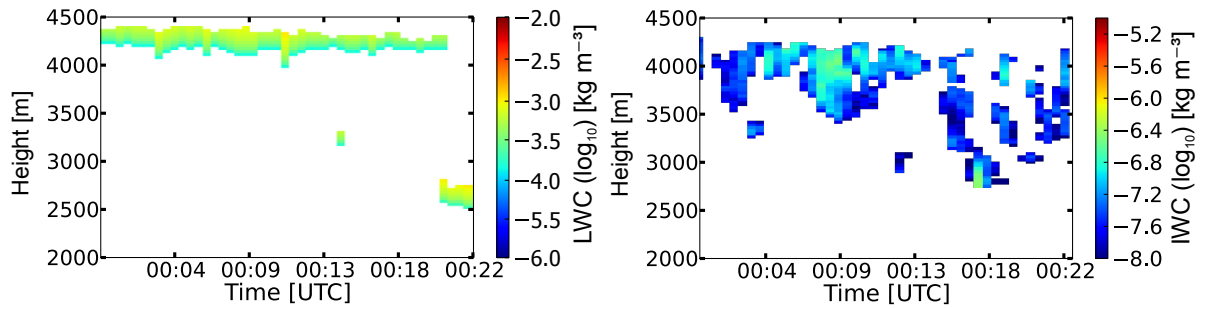


Figure 2: Cloudnet derived water contents for case 1. Left: Liquid water content, right: ice water content (both in logarithmic scale).

74 *butions of the different processes involved in these complex interactions. ...*

75 **Reviewer 1**

76 2. The observations that motivated the selection of these cases, and which are relied
 77 upon, are not adequately shown and their uncertainty properties are not described.
 78 Figure 1b makes a good start at showing case 1 cloud conditions, but other case 1
 79 figures are truncated in time. Please show all five of the following fields between 23:45
 80 and 0:40 for case 1 (providing important context for the narrow 20-minute window
 81 used for the study) and for case 2: lidar backscatter, radar reflectivity, retrieved IWC,
 82 retrieved LWC, retrieved vertical wind. Only the first is shown for the full time range for
 83 case 1. LWC is never shown now. Also please report the stated or estimated uncertainty
 84 properties of IWC, LWC and vertical wind speed. Are there no clear-air vertical wind
 85 retrievals from the Doppler lidar? Please explain why the vertical wind speeds shown in
 86 Figure 2 appear as they do for lidar. Finally, please show plots of the initial soundings
 87 used, including RHI and RH.

88 **Authors**

89 Additional pictures are shown for both cases in the revised version. However, for case
 90 1 full time range is shown only for 2 parameters (RC signal, radar reflectivity, new Fig.
 91 1) because at 0:22 h, a new cloud appears to form at a lower level (compare also humid
 92 layer in profile, Fig. 7) around 3000 m.

93 *... This is supported by Fig. 3 where the cloud radar (right panel) mainly shows parti-*
 94 *cles falling from the top layer. Therefore, particles are mainly moving downwards (green*
 95 *color) and can be identified as ice particles by their size. Only at the very top at about*
 96 *4300 m particles are small enough to still be lifted upwards (yellow colors). The Doppler*
 97 *lidar (left panel), however, shows the motion of small cloud droplets at the predominantly*
 98 *liquid cloud top. Hence, in this plot the cloud-top turbulence becomes visible. ...*

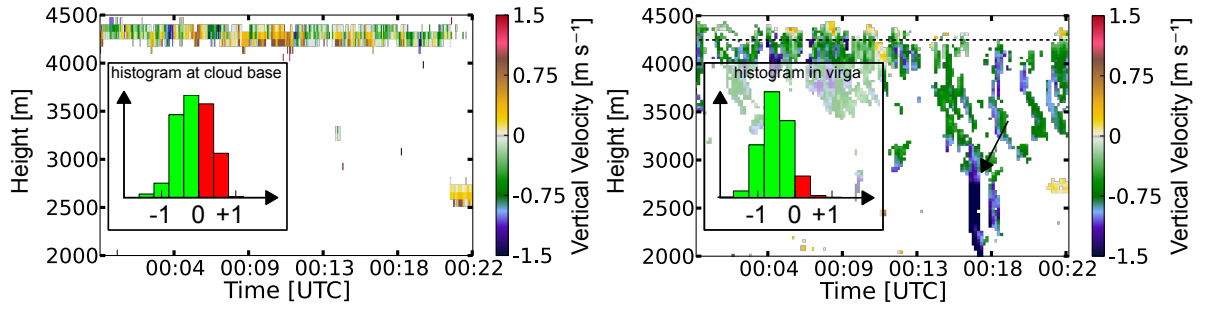


Figure 3: Vertical velocity for case 1. Left: derived from lidar (valid for more numerous smaller droplets at cloud base), right: derived from radar observations (valid for large particles; virgae).

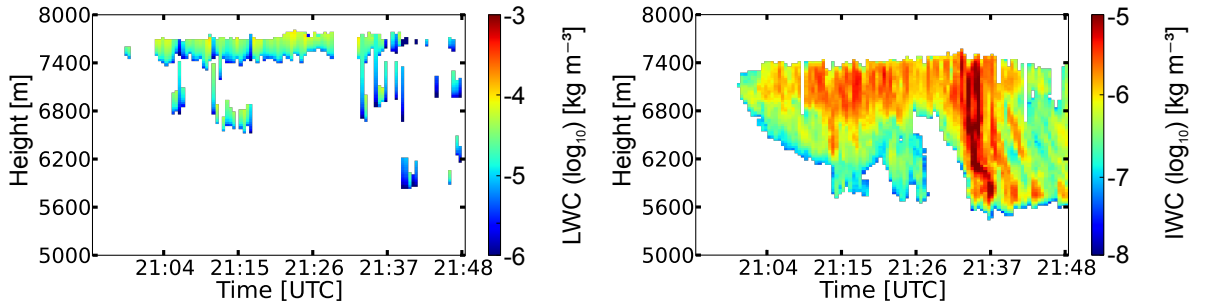


Figure 5: Cloudnet derived water contents for case 2. Left: Liquid water content, right: ice water content (both in logarithmic scale).

99 Accuracy of observations is discussed as follows:

100 Accuracy of the IWC is +/-50 %. For the LWC calculated by the scaled adiabatic
 101 approach the same order of magnitude applies. Vertical wind speeds are measured directly
 102 by evaluation from the recorded cloud radar and Doppler lidar spectra. Errors are +/-
 103 0.15m/s for the cloud radar and +/-0.05m/s for the Doppler lidar. These errors are
 104 mainly due to the pointing accuracy of the two systems.

105 There are no possibilities to derive clear air velocity with a coherent doppler wind lidar,
 106 because this instrument depends on tracer targets like aerosol particles or cloud droplets.
 107 However, clear air motions around a cloud is a very interesting quantity which can, e.g.,
 108 be derived with radar wind profilers. See for example: [http://www.atmos-meas-tech-](http://www.atmos-meas-tech-discuss.net/8/353/2015/amtd-8-353-2015.pdf)
 109 [discuss.net/8/353/2015/amtd-8-353-2015.pdf](http://www.atmos-meas-tech-discuss.net/8/353/2015/amtd-8-353-2015.pdf)

110 Initial soundings (T, rh, rhi) are shown as new Fig. 7.

111 ... *Fig. 7 shows profiles of temperature and relative humidities with respect to liquid*
112 *water and to ice, respectively, for both cases. ...*

113 **Reviewer 1**

114 3. The authors acknowledge that the specification of vertical winds is a controlling
115 parameter, but they do not discuss the general nature of these winds, which seems
116 to be important to understanding the relationship of the model setup to the large-
117 scale conditions. Is the mean vertical wind described large-scale in nature whereas the
118 stochastic components are turbulence? I would expect the updrafts and downdrafts
119 within altocumulus to be driven by cloud-top cooling rather than large-scale winds. In
120 the case that cloud-top cooling-driven turbulence is driving mixing between downdrafts
121 and updrafts, I would expect it to drive the supply of IN. However, the authors state that
122 the mean wind is driving the supply of IN. Does that mean that large-scale convergence
123 is driving the supply of IN to updrafts and downdrafts whereas turbulence does not play
124 a role in the supply of IN?

125 **Authors**

126 We share your statement that cloud-top cooling is an important driver for altocumulus
127 clouds. We consider this effect to be included in the observations as well as in the
128 prescribed vertical velocity.

129 In the paper, we state that the supply of IN is driven by the horizontal exchange with
130 the outer cylinder. The horizontal exchange is driven by the change of vertical wind
131 speed with height (see Eq. (4)). This means that turbulence (which is responsible for
132 the direction of vertical wind speed) plays a major role in IN supply.

133 The mean vertical wind can be considered as large-scale driving force, however, due
134 to the model configuration, the strength of the mean updraft has to be chosen larger
135 than observed.

136 **Reviewer 1**

137 4. The model vertical resolution is 25 m, but what is the size of the inner and outer
138 cylinder? How was it decided how large to make the inner and outer cylindrical coordi-
139 nates? Are results sensitive to the specification of cylinder relative size? Is the inner
140 cylinder considered to be the whole 20-min cloud observed (both updrafts and down-
141 drafts) whereas the outer cylinder is the air surrounding the cloud? If so, how much
142 air surrounding the cylinder? Or is the cylinder specified to be an updraft element size,
143 similar to deep convection studies?

144 **Authors**

145 The radius was chosen to be 100 m for the inner cylinder and 1000 m for the outer
146 cylinder. In an Asai-Kasahara model the ratio of the radius of the inner cylinder to
147 the radius of the outer cylinder is the dominating parameter and the chosen value of

148 1:10 is a typical value for an Asai-Kasahara model setup. The results are sensitive to
149 the radius ratio when the outer cylinder is chosen too small. Then the influence of the
150 inner on the outer cylinder increases and the outer cylinder cannot serve as a proper
151 background any more. However, the geometric configuration of the model is not intended
152 to describe or to match the geometry of the clouds (and cloud-free spaces in between)
153 as observed. It should rather be understood as a possibility to describe a vertically
154 resolved cloud evolution and to provide the possibility of horizontal exchange with a
155 cloud-free background (see also response to reviews 2 and 3). Neither is it intended to
156 directly model the cases presented. They rather should serve as frame to judge whether
157 the model simulations lead to results close enough to reality to apply the model to
158 sensitivity studies. Therefore, the 60 minute model runs are not compared directly to a
159 20 minute period of observations. However, the inner cylinder gives the relevant results
160 for both, updrafts and downdrafts.

161 The manuscript was changed as follows:

162 *... with radii of 100 m and 1000 m, respectively, resulting in a radius ratio of 1:10*
163 *which is typical for this setup. However, the geometric configuration of the model is*
164 *not intended to match the geometry of the clouds (and the cloud-free spaces between*
165 *the clouds) but is rather meant to provide the possibility of horizontal exchange between*
166 *clouds and a cloud-free background. ...*

167 **Reviewer 1**

168 5. Aggregation and riming are neglected? Please provide some literature support for
169 why that would be appropriate or otherwise explain.

170 **Authors**

171 The observed clouds are rather shallow and a large fraction of the ice is formed at/near
172 cloud base which means that there is not that much possibility of ice particles to rime.
173 Aggregation can be neglected due to the rather low ice particle number concentrations for
174 case 1 (relatively small probability of collision between particles) and the relatively low
175 temperatures for case 2 (reducing sticking efficiency). This assumption is corroborated
176 by the findings of Smith et al. (2009, doi:10.1029/2008JD011531) stating that water
177 vapor deposition (and sublimation), balanced by sedimentation are more important than
178 accretional growth.

179 The manuscript was changed accordingly:

180 *... For this case study, collision processes between ice particles and drops (riming)*
181 *and between ice particles and ice particles (accretion) are not taken into account. On*
182 *the one hand, this is to exclude further uncertainties which would be introduced by the*
183 *collision/collection kernel for those interactions, on the other hand, only small or ne-*
184 *glectable effects are expected. Clouds are shallow which means that there is not much*

185 *time for the ice particles to interact with droplets (especially when the ice is prefer-*
186 *entially formed near cloud base and sediments out soon). In addition, for case 1 ice*
187 *particle concentrations are low which highly limits the probability of collisions. At the*
188 *low temperatures of case 2 sticking efficiency is expected to be low. This assumption*
189 *is corroborated by the findings of Smith et al. (2009) stating that water vapor deposi-*
190 *tion (and sublimation), balanced by sedimentation are more important than accretional*
191 *growth. ...*

192 **Reviewer 1**

193 6. (1581/21) M1 and M6 both have lower free troposphere aerosol. Why did you choose
194 M6 for case 1 and M1 for case 2? How did you apportion 1e5/kg aerosol among the
195 three modes?

196 **Authors**

197 For case 2 the upper free troposphere (UFT) aerosol distribution of M1 was used, whereas
198 for case 1 the lower free troposphere aerosol (LFT) of M6 was used. The choice of
199 the aerosol distributions is quite arbitrary, however, one intention was to use M6 LFT
200 measurements with and without a polluted layer for case 1. Nevertheless, the polluted
201 layer run was not reported since Lidar observations showed no polluted layers for case 1.
202 For the UFT, no polluted layers were observed in Petzold et al., therefore, we decided
203 to use M1 from the beginning.

204 We assume that 1e5/kg particles are larger than 250 nm (in radius) according to the
205 parameterization of DeMott et al. to calculate and initialize the temperature-dependent
206 INP field. This has to be considered separately from the AP distributions used for the
207 initialization of the combined AP/drop spectrum. Those are taken as described in the
208 paper cited.

209 **Reviewer 1**

210 7. (1586/6, 1578/4) DeMott et al. (2010) did not analyze measurements colder than -9
211 C, to my knowledge. Did you extrapolate their relationship to colder temperatures? If
212 so, how did you decide at what temperature to stop extrapolating when approaching 0
213 C?

214 **Authors**

215 Yes. DeMott et al. (2010) only shows observations for temperatures below -9 C. We
216 extrapolated the relationship to higher temperatures (-5 C). We did not have to decide
217 where to stop the extrapolation in these case studies since in the model used ice formation
218 by immersion freezing could only take place in the vicinity of drops which were only
219 present at temperatures below -5/-6 C.

220 The manuscript was changed accordingly:

221 ... To cover case 1, the parameterization is extrapolated to -5°C despite the fact that
222 the underlying measurements were only taken at -9°C and below. ...

223 **Reviewer 1**

224 8. (1579/2) Because the relationships in Mitchell et al. (1996) and past literature
225 have been derived from observations over limited size ranges, it is not uncommon to
226 use more than one relationship to represent columns of various sizes (e.g., Sölch et al.
227 QJRMS 136:2074, 2010, table AII). Please provide sufficient information re exactly which
228 relationships you used and over what size ranges for this work to be reproduced.

229 **Authors**

230 We used the relationships in Mitchell et al. (1996) in their Tab. 1 for hexagonal
231 plates and hexagonal columns. The mass-dimension power laws were transformed to
232 aspect ratios for the given shapes. For columns, three size ranges (30 to 100 μm , 100 to
233 300 μm , and above 300 μm in diameter) with different coefficients are given whereas for
234 plates the coefficients are valid for diameters from 15 to 3000 μm .

235 The manuscript was changed accordingly:

236 ... (ranging from 15 to 3000 μm with a single description) and columns (for size ranges
237 of 30 to 100 μm , 100 to 300 μm , and above 300 μm in diameter) are calculated from the
238 mass-dimension power laws ...

239 **Reviewer 1**

240 9. (1575/5) Could preconditioned ice nuclei be nucleated as warm as -1°C
241 or some other temperature limit? Please explain mechanistically how preconditioning
242 could introduce ice nuclei relevant in this study, with reference to literature and relevant
243 temperature range.

244 **Authors**

245 The statement was removed from the text since it was too speculative.

246 **Reviewer 1**

247 10. (1576/30) IWC is shown to 2000 m in Figure 1, which apparently is warmer than 0
248 $^{\circ}\text{C}$ according to the text, which states that IWC extends to only 3000 m. Please clarify.

249 **Authors**

250 Indeed there is no ice detected below 0 $^{\circ}\text{C}$. The IWC is derived by the parameterization
251 of Hogan 2006 which computes IWC as a simple function of radar reflectivity and tem-
252 perature. The equation is mathematically valid for $T > 0^{\circ}\text{C}$, so the usage of this equation
253 has to be restricted to temperatures below 0 $^{\circ}\text{C}$. That restriction was, however, not done

254 properly in this case. The figure was therefore corrected and now shows IWC only up
255 to 0 C.

256 **Reviewer 1**

257 11. What is the model time step used?

258 **Authors**

259 For the dynamics as well as for the microphysics a time step of 1 s is used.

260 The manuscript was changed accordingly:

261 ... *A time step of 1 s was used for the dynamics as well as for the microphysics.*

262 **Reviewer 1**

263 12. (1582/22) It is stated that "ice forms primarily at cloud base". Does this mean that
264 ice is primarily nucleated at cloud base? Cloud base is warmer than cloud top, so I
265 would expect more rapid nucleation at cloud top. Please explain.

266 **Authors**

267 When drops form at cloud base all available INP active at cloud base temperature
268 can contribute to primary ice formation in the immersion mode. The unfrozen droplets
269 are transported further upwards which results in cooling. Nevertheless, if the cloud
270 is relatively shallow (which is the case here) the temperature difference between cloud
271 base and top is rather small. Therefore, the additional number of active INP causing
272 ice nucleation in the upper parts of the cloud remains also relatively small. Therefore,
273 in summary, more ice particles are nucleated near cloud base than near cloud top in the
274 cases presented here.

275 **Reviewer 1**

276 Technical corrections

277 1 (1576/3). Please define TROPOS.

278 TROPOS is the Leibniz-Institute for Tropospheric Research.

279 The manuscript was changed accordingly.

280 **Response to comments of reviewer 2 on**

281 **"Ice phase in Altocumulus Clouds over Leipzig: Remote sensing observa-**
282 **tions and detailed modelling" by Simmel et al.**

283 **<http://www.atmos-chem-phys-discuss.net/15/1573/2015/>**

284 We thank the reviewer for his/her constructive suggestions and for generally accepting
285 the paper when the proposed revisions are realised.

286 New text of the manuscript is cited in *italic*. Revised manuscript with highlighted
287 changes is given as supplement.

288 **Reviewer 2**

289 This paper has great potential as a comparison between modeled and observed mixed
290 phase clouds. Its strengths are the high quality remote observations and the relatively di-
291 rect modeling approach that allows for straightforward implementation and comparison
292 of different ice nucleus (IN) concentrations and ice crystal shapes. The paper stumbles
293 before reaching the finishing line, so I encourage the authors to improve the paper to
294 its potential. There are a number of problems with the analysis and presentation, as
295 detailed below, but these are relatively minor aspects that can be improved with modest
296 effort. The major shortcoming of the paper is the complete absence of comparison be-
297 tween modeled and observed properties in section 5. This is the section where the most
298 interesting science is finally addressed, through variation in IN concentration and ice
299 crystal shape and fall speed. Is it possible to vary these parameters and obtain results
300 that compare with the lidar and radar observations with higher fidelity? And as such,
301 can the suitability of IN parameterization or crystal habit representation be evaluated?
302 As a single example, there is discussion of the "stronger tilting of the virgae" for non-
303 spherical ice (page 1589). This seems like a perfect aspect to compare to observations. It
304 is only one example, and in general, there needs to be a much more thorough and, to the
305 extent possible, quantitative comparison between modeled and observed mixed-phase
306 properties in this section.

307 **Authors**

308 The presentation of observations is extended by showing IWC and LWC for both cases.
309 Comparison between model and observation seems to be difficult for case 1 where the
310 observations are close to the detection limit. Additionally, the INP parameterization of
311 DeMott is rather insensitive to the number of aerosol particles at rather high tempera-
312 tures of -5 C. For case 2 it seems to be clear that either too many INP or non-spherical
313 particles could easily lead to an overestimation of the ice-phase and even the complete
314 depletion of the liquid phase which is in contradiction to the observations.

315 Conclusions about possible ice shapes being consistent with (a) laboratory studies and
316 (b) our observations are drawn in the final section.

317 **Reviewer 2**

318 The following points should also be addressed:

319 - Abstract: “warm temperatures” should be “high temperatures” (air is warm, tem-
320 peratures are high).

321 - Pg 1574 line 22: “attributed the aerosol” should be “attributed to the aerosol”.

322 **Authors**

323 The changes were done according to the suggestion of the reviewer.

324 **Reviewer 2**

325 - Pg 1574 line 25: I do not understand the statement that only biological particles form
326 ice above -15 C. In the parameterization employed, which is mostly describing dust, IN
327 exist at much higher temperatures.

328 **Authors**

329 There is an ongoing discussion of this topic. In laboratory studies, it was shown, that
330 biological material is able to initiate ice at those high temperatures. However, there are
331 at least two possibilities for dust to form ice above -15 C: (a) Pure dust is also able to
332 form ice above -15 C if only enough material (surface) is available. This is a question of
333 detection limits in lab studies (frozen drop fractions). Experiments with large drop on
334 freezing arrays at least hint to this possibility. (b) Dust is mixed with biological material
335 (forming soil dust). Ice formation in this case is triggered by the biological material at
336 least at higher temperatures.

337 ... *One idea is that freezing is caused by soil dust with biological particles dominating*
338 *the freezing behaviour (O’Sullivan et al., 2014) which could explain on the one hand the*
339 *atmospheric abundancy of biological material and on the other hand the relatively high*
340 *freezing temperatures above -15°C of ambient measurements. Seeding from ice clouds*
341 *above can be excluded for the cases presented which means that ice has formed at the*
342 *cloud temperatures observed. ...*

343 **Reviewer 2**

344 - Pg 1575 line 1: should be “to what extent”.

345 **Authors**

346 The changes were done according to the suggestion of the reviewer.

347 **Reviewer 2**

348 - Pg 1575 line 5-6: reference needed for this statement.

349 **Authors**

350 Statement was removed from the text since it was too speculative.

351 **Reviewer 2**

352 - Pg 1576 line 16: define GDAS.

353 - Pg 1576 line 24: “could be observed” should be “was observed”.

354 - Pg 1577 line 1: “an LWP” should be “a LWP”.

355 **Authors**

356 The changes were done according to the suggestion of the reviewer.

357 **Reviewer 2**

358 - Note: I stopped correcting minor grammatical errors after section 2. Authors, please
359 proofread the paper carefully.

360 **Authors**

361 Careful proofreading was done.

362 **Reviewer 2**

363 - Pg 1577, sec 3: Asai-Kasahara type model should be described more thoroughly, e.g.,
364 be clearer on cylindrical geometry, boundary conditions, etc.

365 **Authors**

366 For initialization of the Asia-Kasahara model, only a vertical profile of temperature and
367 humidity is needed (now shown in new Fig. 7). No additional boundary conditions are
368 needed. The radius was chosen to be 100 m for the inner cylinder and 1000 m for the
369 outer cylinder. In an Asai-Kasahara model the ratio of the radius of the inner cylinder
370 to the radius of the outer cylinder is the dominating parameter and the chosen value of
371 1:10 is a typical value for an Asai-Kasahara model setup. The results are sensitive to
372 the radius ratio when the outer cylinder is chosen too small. Then the influence of the

373 inner on the outer cylinder increases and the outer cylinder cannot serve as a proper
374 background any more. However, the geometric configuration of the model is not intended
375 to describe or to match the geometry of the clouds (and cloud-free spaces in between) as
376 observed. It should rather be understood as a possibility to describe a vertically resolved
377 cloud evolution and to provide the possibility of horizontal exchange with a cloud-free
378 background (see also response to reviews 1 and 3).

379 The manuscript was changed accordingly:

380 *... with radii of 100 m and 1000 m, respectively, resulting in a radius ratio of 1:10*
381 *which is typical for this setup. However, the geometric configuration of the model is*
382 *not intended to match the geometry of the clouds (and the cloud-free spaces between*
383 *the clouds) but is rather meant to provide the possibility of horizontal exchange between*
384 *clouds and a cloud-free background. ...*

385 **Reviewer 2**

386 - Sec 3.1.1: Regarding “Immersion freezing occurs as soon as liquid drops above a
387 certain size limit are present”, why is there a drop size dependence? Freezing probability
388 should be related to IN properties, not to volume of drop.

389 **Authors**

390 One possible way of the drop volume to influence freezing is the concentration of solved
391 chemical species which may lead to a freezing point depression in the case of relative
392 large aerosol particles with relatively little water mass. The size limit is intended to make
393 sure that there are supercooled drops available for freezing and to avoid the freezing of
394 aerosol particles which are present in the same joint spectral liquid-phase field.

395 *... The drop size threshold was chosen to restrict freezing to droplets and to prevent*
396 *(large) non-activated aerosol particles at high relative humidity (but subsaturated wrt*
397 *water) outside the cloud from freezing. ...*

398 **Reviewer 2**

399 - Sec. 3.2.1 and Fig 5: What is the advantage of using a stochastic forcing for vertical
400 velocity? It seems to only add complexity, with no obvious illumination of new physics.
401 Why not force with a deterministic, e.g., sinusoidal, vertical velocity, for example?

402 **Authors**

403 A simpler profile was tested (constant up- and downdrafts for given times with short
404 linearly interpolated transitions between both), however, it appears that this more com-
405 plex stochastic forcing gives more realistic results and better shows the variety of cloud’s
406 LWC and IWC since it better matches the temporal patterns of the updraft. Addition-
407 ally, the more often changes between up- and downdrafts on smaller time scales provide

408 a certain horizontal exchange between inner and outer cylinder which is important for
409 the supply of fresh INP.

410 **Reviewer 2**

411 - Pg 1583 line 27: I think “presence time” is clearer as “residence time”.

412 **Authors**

413 The change was done according to the suggestion of the reviewer.

414 **Reviewer 2**

415 - Sec 4: Comparison with figures and reported results is not straightforward: for
416 example, figures are in g/kg, observations are in kg/m^3 . Please be consistent.

417 **Authors**

418 To be consistent, all model results were changed to g/m^3 .

419 **Reviewer 2**

420 - Fig 1: Left panel should be labeled as \log_{10} of IWC.

421 **Authors**

422 The change was done according to the suggestion of the reviewer.
423 CHECK

424 **Reviewer 2**

425 - Fig 1: What is the purpose of the dashed box? Maybe I missed it in the text, but
426 it should also be specified in the caption.

427 **Authors**

428 Fig. 1a and 1b show different height and time ranges. Since Fig. 1b shows a larger
429 part of the data, the dashed box indicates the region shown in Fig. 1a. This was clarified
430 in the revised manuscript (new Fig. 1).

431 CHECK

432 **Reviewer 2**

433 - Figs 6, 8, 10, 12: How useful are these comparisons? The differences between the
434 panels are so small that it is not clear to me that they need to be presented graphically.
435 The numerical results such as max LWMR and max IWMR may be adequate, unless
436 details of the plots are specifically discussed in the text.

437 **Authors**

438 In our opinion, there are quite significant differences between the cases shown which
439 were already mentioned in the manuscript. In Fig. 6, the main differences can be
440 seen in the liquid phase (contours), but also in the ice phase (increase of the ice phase
441 cloud base). Fig. 8 shows substantial differences in both phases, Fig. 10 again shows
442 differences mainly in the liquid phase. Fig. 12 (upper panels) show large differences in
443 both phases, whereas Fig. 12 (lower panels) illustrates the different timing due to the
444 changed forcing.

445 **Reviewer 2**

446 - Figs 6, 8, 10, 12, 14, 15, 17, 18: Maximum ice and liquid water values are reported
447 with 7 significant digits. It cannot be that such accuracy is valid. (Also note that there
448 is some inconsistency in using max LWMR versus max. drop water, etc.).

449 **Authors**

450 There is no valid 7 digit accuracy. This was changed to 3 significant digits. In the
451 revised paper, LWC and IWC are used consistently.

452 **Reviewer 2**

453 - Figs 15 and 18: The captions state that liquid is denoted by color and ice water
454 mass is denoted by contours. That seems to be backwards.

455 **Authors**

456 Yes. This was changed.

457 **Reviewer 2**

458 - Fig 16: In the bottom of the left panel, please confirm that all lines are plotted (i.e.,
459 are they identical and cannot be distinguished?)

460 **Authors**

461 All lines are identical. Compared to the liquid fraction, the ice fraction is so small
462 that changes as modelled in the sensitivity runs are too small to affect the liquid phase
463 considerably (compare LWMR — now LWC — maxima in Table 3 of case 1).

464 **Response to comments of reviewer 3 on**

465 **"Ice phase in Altocumulus Clouds over Leipzig: Remote sensing observa-**
466 **tions and detailed modelling"** by Simmel et al.

467 <http://www.atmos-chem-phys-discuss.net/15/1573/2015/>

468 We thank the reviewer for his/her constructive suggestions and for generally accepting
469 the paper when the proposed revisions are realised.

470 New text of the manuscript is cited in *italic*. Revised manuscript with highlighted
471 changes is given as supplement.

472 **Reviewer 3**

473 General comments: The authors simulate two mixed-phase cloud layers that were ob-
474 served by remote sensing. However, the dynamical model used is unsophisticated, and
475 key observations needed to initialize, force, and validate the simulations are unavailable.
476 For instance, the study concludes that IWP is sensitive to IN number, but there are
477 no IN measurements to assess how much IN number should be varied in the sensitivity
478 study. Hence the conclusions must necessarily be regarded as tentative. Furthermore,
479 only two cloud cases are examined, limiting the conclusions' generality. If the authors
480 wish to simulate a case study, then I recommend that they choose a more complete
481 dataset to simulate, one that uses more accurate (e.g. in situ) measurements. Also, I
482 recommend that they use a more sophisticated model (e.g. LES). If the authors wish
483 to do an observational study, then I recommend that they exploit the instruments they
484 have. Given the facts that the set of instruments is incomplete, that none are in situ,
485 but that they can be run continuously, the instruments seem better suited to assessing
486 climatological relationships between variables. If, instead, the authors wish to invest the
487 time to maximize the usefulness of the present study, I would attempt to better quantify
488 the statement "the liquid phase is mainly determined by the model dynamics (location
489 and strength of vertical velocity) whereas the ice phase is much more sensitive to the
490 microphysical parameters (ice nuclei (IN) number, ice particle shape)." In particular, in-
491 stead of varying w_{ave} from 0.1 to 0.4 m/s, I would vary it by "observed" values taken
492 from obs or reanalyses or the literature. Instead of varying N_{AP} by a factor of 10, vary
493 it by the suitable range given by values in the literature. That would provide a better
494 sense of the practical sensitivity of LWP and IWP to w_{ave} versus N_{AP} . Consider
495 doing likewise for the other sensitivity experiments.

496 **Authors**

497 The general idea of the paper is to use a two step approach: In the first step, the
498 model is used to simulate a cloud which is close to the one observed (in terms of model
499 input – e.g., temperature/humidity profile, vertical velocity – and output – e.g., cloud

500 evolution, liquid and ice phase). If this is done successfully, the model can be used for
501 a second step which is a sensitivity study with respect to certain parameters. This
502 sensitivity study is done within the 'model world' by varying the respective input data
503 (e.g., INP number) and comparing the results.

504 The variation of N_{AP} is in the range of the observations which are the basis of
505 the parameterization used. Only the very high concentrations were omitted since no
506 polluted layers were observed by the lidar.

507 It must be stated that the variation of the w_{ave} is caused by the model configuration:
508 If w_{ave} is chosen to be smaller than about 0.1 m/s the model will not be able to reach
509 supersaturation and to form a cloud due to the horizontal exchange with the background.
510 On the other hand, if w_{ave} is chosen much larger than 0.4 m/s, the downdrafts will be
511 too weak and too short to lead to cloud-free spaces in between the clouds.

512

513 **Reviewer 3**

514 Specific comments:

515 The abstract is well written, but the introductory section could more clearly introduce
516 the main issues that will be addressed in the paper. What is the gap in knowledge, and
517 how will it be addressed in the subsequent sections?

518 **Authors**

519 The underlying topic is mixed-phase microphysics and the interaction between the
520 three phases of water. It is well-known that due to the different saturation pressure
521 of water vapor with respect to liquid water and ice, a mixed-phase cloud is in a non-
522 equilibrium state which, nevertheless, may lead to a quasi-steady existence (e.g., Korolev
523 and Field, 2008, JAS). For this purpose, a bin model is suited well, since condensa-
524 tional/depositional growth is not only described by saturation adjustment but by a
525 detailed description of sub-/supersaturation of each size bin resulting in different growth
526 rates. This automatically results in a very detailed description of the Wegener-Bergeron-
527 Findeisen (WBF) process which drives the phase interaction.

528 The main drivers for this phase transfer are vertical velocity (leading to supersatu-
529 ration and subsequent droplet formation) and ice particle formation and growth (WBF
530 starts) leading to sedimentation of the typically fast growing ice particles (WBF ends
531 due to removal of ice). The motivation of this work is to shed more light on the relative
532 contributions of the different processes involved in these complex interactions (see also
533 response to review 1).

534 *According to Warren et al. (1998a,b) altocumulus and altostratus clouds together cover*
535 *22 % of the earth's surface. For single-layered altocumulus clouds, ...*

536 ... This was previously reported from Fleishauer et al. (2002) and Carey et al. (2008).
537 Fleishauer et al. (2002) also emphasized a lack of significant temperature inversions or
538 wind shears as a major feature of these clouds. Kanitz et al. (2011) show that the ratio of
539 ice-containing clouds increases with decreasing temperature. However, the numbers are
540 different for different locations with similar dynamics but with different aerosol burden,
541 e.g., at northern and southern midlatitudes, underlining the question for the influence
542 of ice-nucleating particles (INP). ...

543 ... However, despite its important contribution, ice nucleation does not determine
544 the entire microphysics of mixed-phase clouds alone. It is rather the complex trans-
545 fer between the three phases of water: water vapor, liquid water and ice described by
546 the Wegener-Bergeron-Findeisen (WBF) mechanism (Wegener, 1911; Bergeron, 1935;
547 Findeisen, 1938). It is well-known that due to the different saturation pressures of water
548 vapor with respect to liquid water and ice, a mixed-phase cloud is in a non-equilibrium
549 state which, nevertheless, may lead to a quasi-steady existence (Korolev and Field, 2008).
550 The main drivers for this phase transfer are vertical velocity (leading to supersaturation
551 and subsequent droplet formation) and ice particle formation and growth (WBF starts
552 leading to sedimentation of the typically fast growing ice particles (WBF ends due to
553 removal of ice). The motivation of this work is to shed more light on the relative contri-
554 butions of the different processes involved in these complex interactions. ...

555 Reviewer 3

556 p. 1576: “The liquid part of the cloud extends from about 4250 to 4450 m height at
557 temperatures of about -6 C according to the GDAS reanalysis data for Leipzig.” Some
558 of the discussion relates to the temperature at which various IN are active. Therefore,
559 it is of relevance to know: What are the error bars on the temperature measurement? I
560 wouldn’t expect a reanalysis to be terribly accurate.

561 Authors

562 Temperature errors of the GDAS data compared to radiosonde profiles over Leipzig
563 has been determined to be +/-1K during the DRIFT-project by Patric Seifert (see
564 <http://onlinelibrary.wiley.com/doi/10.1029/2009JD013222/pdf>). These errors seem to
565 be sufficiently small to allow for a strong connection between temperature (as deduced
566 from GDAS reanalysis) and potential ice formation processes.

567 Reviewer 3

568 p. 1577: “For the model studies an Asai–Kasahara type model is used (Asai and
569 Kasahara, 1967). The model geometry is axisymmetric and consists of an inner and
570 an outer cylinder.” By today’s standards, the Asai-Kasahara model is crude. Instead, I
571 recommend using a large-eddy simulation (LES) model. These days, LES are affordable
572 and easy to configure. If not LES, then I recommend trying a prescribed dynamics model
573 like the Kinematic Driver (KiD) model, because it will provide flexibility and control.

574 **Authors**

575 Maybe the term "Asai-Kasahara" is misunderstood. As it is explained, vertical dy-
576 namics is prescribed which to our understanding is rather similar to the KiD model. Only
577 the model geometry assumption (cylinder-symmetric with an inner and an outer cylin-
578 der) and the exchange between the cylinders (see Eq. (4)) relates to the Asai-Kasahara
579 model.

580 However, the geometric configuration of the model is not intended to describe or to
581 match the geometry of the clouds (and cloud-free spaces in between) as observed. It
582 should rather be understood as a possibility to describe a vertically resolved cloud evo-
583 lution and to provide the possibility of horizontal exchange with a cloud-free background
584 (see also response to reviews 1 and 2).

585 *... However, the geometric configuration of the model is not intended to match the ge-*
586 *ometry of the clouds (and the cloud-free spaces between the clouds) but is rather meant to*
587 *provide the possibility of horizontal exchange between clouds and a cloud-free background.*

588 ...

589 *... However, in contrast to other Asai-Kasahara model studies, updrafts are not initial-*
590 *ized by a heat and/or humidity pulse in certain layers for a given period of time. Instead,*
591 *vertical velocity (updrafts and downdrafts) in the inner cylinder is prescribed, which is*
592 *more similar to a kinematic model like the Kinematic Driver Model KiD (Shipway and*
593 *Hill, 2012). In that way dynamics can be controlled to make sure that it is close to the*
594 *observations. ...*

595 **Reviewer 3**

596 p. 1577: "Since during the above mentioned observations no measurements of the IN
597 are available, the parameterization of DeMott et al. (2010) is used assuming that all
598 IN are active in the immersion freezing mode." The observations needed to address the
599 scientific questions are lacking. Consider focusing your efforts on addressing a question
600 that your instruments are better positioned to answer.

601 **Authors**

602 In general, ambient INP measurements are sparse and typically not available for long-
603 term observations. We do not think that this fact should deter us from investigating
604 those cases. It is a common approach to use certain assumptions (here about INP) and
605 to check how the model results based on those assumptions compare to observations.
606 Additionally, sensitivity studies are carried out to check how important the respective
607 parameter is for the whole situation.

608 **Reviewer 3**

609 p. 1579: "For case 1, profiles from both methods show a similar general behaviour
610 but the radiosonde profile of Meiningen measured at 00:00 UTC is used since it pro-

611 vides a finer vertical resolution than the GDAS reanalysis data. However, for case 2
612 the Meiningen RS profile misses the humidity layer at the level where the clouds were
613 observed and, therefore, GDAS reanalysis data for Leipzig at 21:00 UTC were chosen.”
614 Apparently, the observations are too inaccurate to initialize the simulations.

615 **Authors**

616 The Meiningen profile was not representative for Leipzig for case 2. Therefore, the
617 GDAS profile was chosen as a substitute. Despite the coarser height resolution, cloud
618 formation was triggered in the model when vertical updrafts similar to the observed
619 ones were prescribed. Again, we have to emphasize that the aim of the study was not
620 to model the observed cases in detail but more to obtain reasonable model results that
621 allow for sensitivity studies which are in turn transferable to the ”real world”.

622 **Reviewer 3**

623 p. 1581: “Since no in situ aerosol measurements are available, literature data is used.”
624 The dataset is inadequate for the purpose of studying sensitivity to IN.

625 **Authors**

626 The Lidar shows that no dust layers or similar pronounced features concerning aerosol
627 could be observed. Therefore, we consider it reasonable to use those literature data. The
628 aim of the study is not to study sensitivity of the clouds with respect to INP on the
629 basis of observations. If this was the case, we would have to have measurements of both,
630 cloud ice phase as well as INP, to obtain e.g., statistical correlations between both data
631 sets. However, we use a two step approach mentioned above which allows us to perform
632 the sensitivity study in the ’model world’.

633 **References**

- 634 Bergeron, T.: On the physics of clouds and precipitation, in: *Proces verbaux de*
635 *l’association de Meteorologie*, pp. 156–178, International Union of Geodesy and Geo-
636 *physics*, Lisboa, Portugal, 1935.
- 637 Carey, L. D., Niu, J., Yang, P., Kankiewicz, J. A., Larson, V. E., and Vonder Haar,
638 T. H.: The Vertical Profile of Liquid and Ice Water Content in Midlatitude Mixed-
639 Phase Altocumulus Clouds, *J. Appl. Meteorology and Climate*, 47, 2487–2495, 2008.
- 640 Findeisen, W.: *Kolloid-meteorologische Vorgänge bei Niederschlagsbildung*, *Meteorolog.*
641 *Z.*, 55, 121–133, 1938.
- 642 Fleishauer, R. P., Larson, V. E., and Vonder Haar, T. H.: Observed Microphysical
643 Structure of Midlevel, Mixed-Phase Clouds, *J. Atmos. Sci.*, 59, 1779–1804, 2002.

- 644 Kanitz, T., Seifert, P., Ansmann, A., Engelmann, R., Althausen, D., Casiccia, C., and
645 Rohwer, E. G.: Contrasting the impact of aerosols at northern and southern midlat-
646 itudes on heterogeneous ice formation, *Geophysical Res. Letters*, 38, L17802, URL
647 doi:10.1029/2011GL048532, 2011.
- 648 Korolev, A. and Field, P. R.: The Effect of Dynamics on Mixed-Phase Clouds: Theo-
649 retical Considerations, *J. Atmos. Sci.*, 65, 66–86, 2008.
- 650 O’Sullivan, D., Murray, B. J., Malkin, T. L., Whale, T. F., Umo, N. S., Atkinson, J. D.,
651 Price, H. C., Baustian, K. J., Browse, J., and Webb, M. E.: Ice nucleation by fer-
652 tile soil dusts: relative importance of mineral and biogenic components, *Atmospheric*
653 *Chemistry and Physics*, 14, 1853–1867, URL doi:10.5194/acp-14-1853-2014, 2014.
- 654 Shipway, B. J. and Hill, A. A.: Diagnosis of systematic differences between multiple
655 parametrizations of warm rain microphysics using a kinematic framework, *Q. J. R.*
656 *Meteorol. Soc.*, 138, 2196–2211, URL doi:10.1002/qj.1913, 2012.
- 657 Smith, A. J., Larson, V. E., Niu, J., Kankiewicz, J. A., and Carey, L. D.: Processes that
658 generate and deplete liquid water and snow in thin midlevel mixed-phase clouds, *J.*
659 *Geophys. Res.*, 114, D12203, URL doi:10.1029/2008JD011531, 2009.
- 660 Warren, S. G., Hahn, C. J., London, J., Chervin, R. M., and Jenne, R.: Global distri-
661 bution of total cloud cover and cloud type amount over land, Tech. Rep. Tech. Note
662 TN-317 STR, NCAR, 1998a.
- 663 Warren, S. G., Hahn, C. J., London, J., Chervin, R. M., and Jenne, R.: Global distri-
664 bution of total cloud cover and cloud type amount over the ocean, Tech. Rep. Tech.
665 Note TN-317 STR, NCAR, 1998b.
- 666 Wegener, A.: *Thermodynamik der Atmosphäre*, J. A. Barth Verlag, 1911.

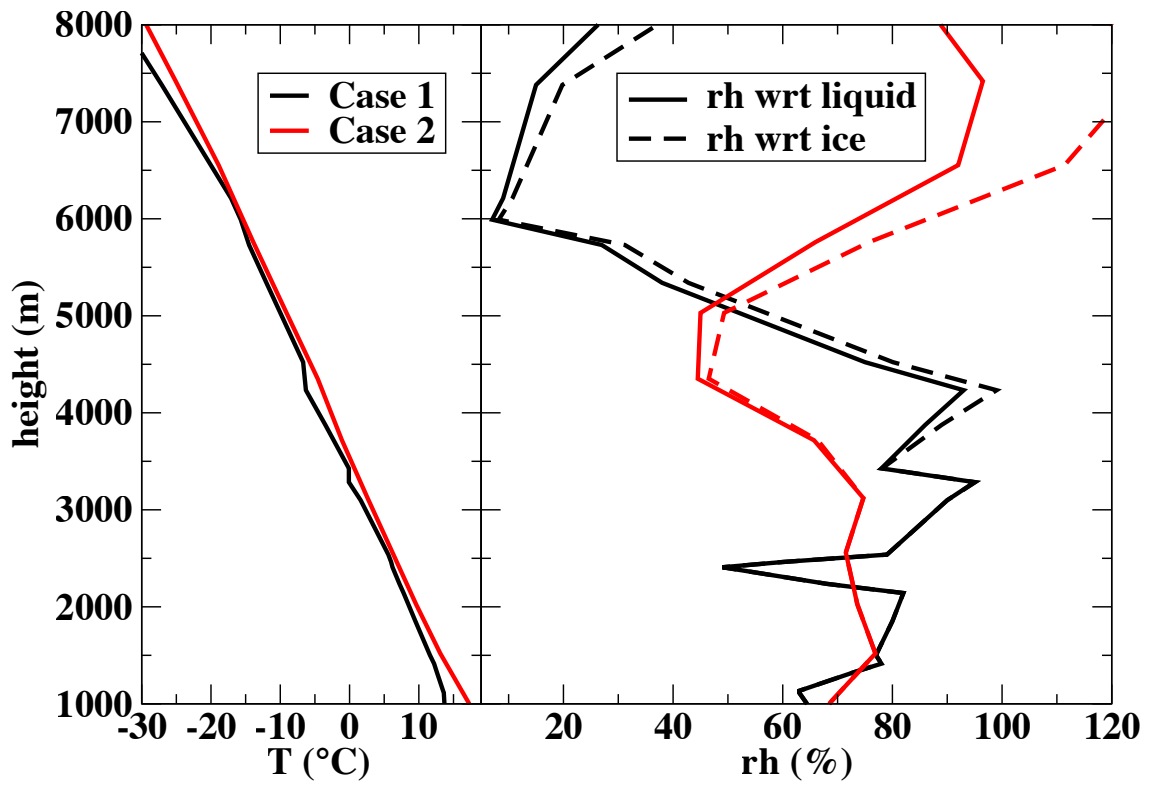


Figure 7: Vertical profiles of temperature (left) and relative humidity (right) with respect to liquid water (full lines) and ice (dashed lines) based on a radiosonde observation (Meiningen) for case 1 (black) and from GDAS (grid point Leipzig) for case 2 (red).

Ice phase in Altopcumulus Clouds over Leipzig: Remote sensing observations and detailed modelling

Martin Simmel¹, Johannes Bühl¹, Albert Ansmann¹, and Ina Tegen¹

¹TROPOS, Leibniz Institute for Tropospheric Research, Permoser Str. 15, 04318 Leipzig, Germany

Correspondence to: Martin Simmel
(simmel@tropos.de)

Abstract. The present work combines remote sensing observations and detailed cloud modeling to investigate two altopcumulus cloud cases observed over Leipzig, Germany. A suite of remote sensing instruments was able to detect primary ice at rather warm-high temperatures of -6°C . For comparison, a second mixed phase case at about -25°C is introduced. To further look into the details of cloud microphysical processes a simple dynamics model of the Asai-Kasahara type is combined with detailed spectral microphysics forming the model system AK-SPECS. Vertical velocities are prescribed to force the dynamics as well as main cloud features to be close to the observations. Subsequently, sensitivity studies with respect to ice microphysical parameters are carried out with the aim to quantify the most important sensitivities for the cases investigated. For the cases selected, the liquid phase is mainly determined by the model dynamics (location and strength of vertical velocity) whereas the ice phase is much more sensitive to the microphysical parameters (ice nuclei (IN) nucleating particle (INP) number, ice particle shape). The choice of ice particle shape may induce large uncertainties which are in the same order as those for the temperature-dependent IN-INP number distribution.

1 Introduction

Altopcumulus clouds. According to Warren et al. (1998a,b) altopcumulus and altostratus clouds together cover 22 % of the earth's surface. For single-layered altopcumulus clouds, observations by Buehl et al. (2013) show the typical feature with a maximum of liquid water in the upper part of the cloud (increasing with height) and an ice maximum in the lower part of the cloud, mostly below liquid cloud base down in the virgae. This was previously reported from Fleishauer et al. (2002) and Carey et al. (2008).

Fleishauer et al. (2002) also emphasized a lack of significant temperature inversions or wind shears as a major feature of these clouds. Kanitz et al. (2011) show that the ratio of ice-containing clouds increases with decreasing temperature. However, the numbers are different for different locations with similar dynamics but with different aerosol burden, e.g., at northern and southern midlatitudes, underlining the question for the influence of ice-nucleating particles (INP). The observations with the highest temperatures are close to the limit at which the best atmospheric ice nuclei are known to nucleate ice in the immersion mode. This can only be attributed to the aerosol particles which are formed out of or at least contain biological material such as bacteria (Hartmann et al., 2013), fungi, or pollen. This is corroborated by the review of Murray et al. (2012) stating that only biological particles are known to form ice above -15°C . However, these observations are from laboratory studies and it is still unclear whether or to which-what extent these extremely efficient ice nuclei are abundant in atmosphere, especially above the boundary layer. One idea is that freezing is caused by soil dust with biological particles dominating the freezing behaviour (O'Sullivan et al., 2014) which could explain on the one hand the atmospheric abundance of biological material and on the other hand the relatively high freezing temperatures above -15°C of ambient measurements. Seeding from ice clouds above can be excluded for the cases presented ; however, preconditioning of ice nuclei (IN) could be a reason for these high ice activation temperatures - which means that ice has formed at the cloud temperatures observed.

Ice nucleation still is a large source of uncertainty in cloud modeling. Recently, several studies use combinations of vertically fine resolved models with rather detailed representation of the ice nucleation processes. Often, wave clouds are used as comparison since they represent rather ideal condi-

tions when they are not influenced by ice seeding from layers above. Field et al. (2012) apply a 1D kinematic model with bulk microphysics but prognostic ~~IN-INP~~. Eidhammer et al. (2010) use a Lagrangian parcel model for the comparison of the ice nucleation schemes of Phillips et al. (2008) and DeMott et al. (2010) under certain constraints. A 1D column model with a very detailed 2D spectral description of liquid and ice phase is employed by Dearden et al. (2012). Sun et al. (2012) use a 1.5D model with spectral microphysics for shallow convective clouds for a sensitivity study of immersion freezing due to bacteria and its influence on precipitation formation.

Most ice microphysics descriptions in models lack from the fact that ice nuclei are not represented as a prognostic variable. These models diagnose the number of ice particles based on thermodynamical parameters such as temperature and humidity (MEYERS et al., 1992) and are, therefore, not able to consider whether ~~IN-INP~~ were already activated at previous time steps in the model.

However, despite its important contribution, ice nucleation does not determine the entire microphysics of mixed-phase clouds alone. It is rather the complex transfer between the three phases of water: water vapor, liquid water and ice described by the Wegener-Bergeron-Findeisen (WBF) mechanism (Wegener, 1911; Bergeron, 1935; Findeisen, 1938).

It is well-known that due to the different saturation pressures of water vapor with respect to liquid water and ice, a mixed-phase is in a non-equilibrium state which, nevertheless, may lead to a quasi-steady existence (Korolev and Field, 2008). The main drivers for this phase transfer are vertical velocity (leading to supersaturation and subsequent droplet formation) and ice particle formation and growth (WBF starts) leading to sedimentation of the typically fast growing ice particles (WBF ends due to removal of ice). The motivation of this work is to shed more light on the relative contributions of the different processes involved in these complex interactions.

The paper is structured as follows. Section 2 describes the remote sensing observations of two mixed-phase altocumulus cloud cases above Leipzig. The dynamical model as well as the process descriptions and initial data used for this study are specified in section 3. Section 4 refers to changes in the dynamic parameters of the model to identify base cases ~~–The results for the which describe the observations sufficiently well to perform~~ sensitivity studies with respect to ~~the microphysical parameters~~ microphysical parameters. The results for those sensitivity studies are presented in section 5 and section 6 closes with a discussion of the results.

2 Remote sensing observations

Altocumulus and altostratus clouds are regularly observed with the Leipzig Aerosol and Cloud Remote Observations

System (LACROS) at [the Leibniz Institute for Tropospheric Research TROPOS](#). LACROS combines the capabilities of Raman/depolarization lidar (Althausen et al., 2009), a MIRA-35 cloud radar (Bauer-Pfundstein and Görsdorf, 2007), a Doppler lidar (Bühl et al., 2012), a microwave radiometer, a sun-photometer and a disdrometer to measure height-resolved properties of aerosols and clouds. The Cloudnet framework (Illingworth et al., 2007) is used to derive microphysical parameters like liquid-water content (Pospichal et al., 2012) or ice-water content (Hogan et al., 2006). The following two cases have been selected to illustrate this variety and to serve as examples to be compared to model results.

2.1 Case 1: Warm mixed-phase cloud

One of the warmest mixed-phase clouds within the data set was observed on 17 September 2011 between 00:00 and 00:22 UTC (see Fig. ?? 1). The liquid part of the cloud extends from about 4250 m to 4450 m height at temperatures of about -6°C according to the GDAS (Global Data Assimilation System) reanalysis data for Leipzig. ~~Liquid water~~–Liquid water content (LWC) is between 0.1 g/m^{-3} to 1 g/m^{-3} whereas ice water content (IWC) is about 3–4 orders of magnitude smaller and reaches its maximum value within the virgae (see Fig. 2). Liquid water path (LWP) measured by a microwave radiometer varies between 20 and 50 g/m^2 (mostly about 25 g/m^2) whereas ice water path (IWP) is only slightly above the detection limit of about 0.01 g/m^2 implying a rather large uncertainty with correspondingly large error bars. Virgae (falling ice) are observed down to about 3000 m, which is close to the 0°C level. This is supported by Fig. 3 where the cloud radar (right panel) mainly shows particles falling from the top layer. Therefore, particles are mainly moving downwards (green color) and can be identified as ice particles by their size. Only at the very top at about 4300 m particles are small enough to still be lifted upwards (yellow colors). The Doppler lidar (left panel), however, shows the motion of small cloud droplets at the predominantly liquid cloud top. Hence, in this plot the cloud-top turbulence becomes visible. Vertical windspeeds range from about -1.5 m/s to 1.0 m/s with pdf maxima at -0.5 m/s and 0.5 m/s , respectively (Fig. ?? 3).

2.2 Case 2: Colder mixed-phase cloud

A much colder case ~~could be~~ was observed on 2 August 2012 between 21:00 UTC and 21:40 UTC (see Fig. ?? 4). Liquid water was measured around 7500 m at about -25°C with ~~an~~–a LWP between 10 and 30 g/m^2 ~~–and a LWC of up to~~ 0.1 g/m^{-3} which is much smaller than for case 1. As can be expected due to the lower temperature, the ice phase was much more massive than in case 1 and reached down to about 5500 m with an IWP of about $1\text{--}10\text{ g/m}^2$ ~~–and an IWC of up to~~ 0.01 g/m^{-3} which means that in some parts of the cloud,

ice and liquid water reach the same order of magnitude (see Fig. 5). Vertical wind speeds were in the same range as for the warmer case described above (Fig. 6).

Accuracy of the IWC is $\pm 50\%$. For the LWC calculated by the scaled adiabatic approach the same order of magnitude applies. Vertical wind speeds are measured directly by evaluation from the recorded cloud radar and Doppler lidar spectra. Errors are ± 0.15 m/s for the cloud radar and ± 0.05 m/s for the Doppler lidar. These errors are mainly due to the pointing accuracy of the two systems.

3 Model Description and initialization

For the model studies an Asai-Kasahara type model is used (Asai and Kasahara, 1967). The model geometry is axisymmetric and consists of an inner and an outer cylinder with radii of 100 m and 1000 m, respectively, resulting in a radius ratio of 1:10 which is typical for this setup. However, the geometric configuration of the model is not intended to match the geometry of the clouds (and the cloud-free spaces between the clouds) but is rather meant to provide the possibility of horizontal exchange between clouds and a cloud-free background.

The vertical resolution is constant with height and is chosen to be $\Delta z = 25$ m to give a sufficient resolution of the cloud layer and to roughly match the vertical resolution of the observations. In contrast to a parcel model, the vertically resolved model grid allows for a description of hydrometeor sedimentation. This is important especially for the fast growing ice crystals to realistically describe their interaction with the vapor and liquid phase (Bergeron-Findeisen Wegener-Bergeron-Findeisen process). A time step of 1 s was used for the dynamics as well as for the microphysics.

However, in contrast to other Asai-Kasahara model studies, updrafts are not initialized by a heat and/or humidity pulse in certain layers for a given period of time. Instead, vertical velocity (updrafts and downdrafts) in the inner cylinder is prescribed, which is more similar to a kinematic model like the Kinematic Driver Model KiD (Shipway and Hill, 2012). In that way dynamics can be controlled to make sure that it is close to the observations.

The cloud microphysics is described by the mixed-phase spectral microphysics module SPECS (Simmel and Wurzlner, 2006; Diehl et al., 2006). SPECS provides a joint spectrum for the liquid phase (soluble wetted aerosol particles as well as cloud and rain drops) and one spectrum for the ice phase.

For this case study, collision processes between ice particles and drops (riming) and between ice particles and ice particles (accretion) are not taken into account. On the one hand, this is to exclude further uncertainties which would be introduced by the collision/collection kernel for those interactions, on the other hand, only small or neglectable effects are expected. Clouds are shallow which means that

there is not much time for the ice particles to interact with droplets (especially when the ice is preferentially formed near cloud base and sediments out soon). In addition, for case 1 ice particle concentrations are low which highly limits the probability of collisions. At the low temperatures of case 2 sticking efficiency is expected to be low. This assumption is corroborated by the findings of Smith et al. (2009) stating that water vapor deposition (and sublimation), balanced by sedimentation are more important than accretional growth.

3.1 Description of ice microphysics

In the following, the differences in the description of the microphysics compared to Diehl et al. (2006) are described.

3.1.1 Immersion freezing

For this study, immersion freezing is assumed to be the only primary ice formation process. Since during the above mentioned observations no *in situ* measurements of the IN-INP are available, the parameterization of DeMott et al. (2010) is used assuming that all IN-INP are active in the immersion freezing mode. The parameterization of DeMott et al. (2010) is based on an empirical relation of IN-INP and the number of aerosol particles with radii > 250 nm ($N_{AP,r>250nm}$). To cover case 1, the parameterization is extrapolated to -5°C despite the fact that the underlying measurements were only taken at -9°C and below. As base case $N_{AP,r>250nm} = 10^5 \text{ kg}^{-1}$ air is used as input data for the parameterization resulting in about 0.01 active IN-INP per liter for -6°C (case 1) and about 0.5 IN-INP per liter for -25°C (case 2), respectively, at standard conditions. This corresponds to a relatively low number of larger aerosol particles but is well within the range observed by DeMott et al. (2010).

For the potential IN-INP a prognostic temperature resolved field with 20 temperature bins with a resolution of 1 K is introduced into SPECS. It ranges from -5°C to -25°C to cover the temperature range for the selected cases and can easily be changed for other case studies. This is a simplified version of the method used by Fridlind et al. (2007). The potential IN-INP field is initially defined in every grid cell (layer) and is transported vertically with the given up/downdrafts and horizontally exchanged between inner and outer cylinder in the same way as the other hydrometeor fields (drops and ice crystals). Immersion freezing occurs as soon as liquid drops above a certain size limit are present and the temperature of a certain potential IN-INP bin is reached. Then the respective amount of drops freezes (if available) instantaneously and is transferred from the liquid to the frozen spectrum. If more drops larger than the size threshold of $10 \mu\text{m}$ than active IN-INP are present, the IN-INP are distributed evenly over all drop size bins above the threshold value. The drop size threshold was chosen to restrict freezing to droplets and to prevent (large) non-activated aerosol particles at high relative humidity (but subsaturated

275 wrt water) outside the cloud from freezing. If ice crystals 325
melt below the freezing level, they contribute to the poten-
tial ~~IN-INP~~ field at that level.

3.1.2 Ice particle shape

280 It is well known that ice particle shape highly influences wa-
ter vapor deposition (described by changing the capacitance
of the particle) as well as terminal fall velocity of the ice
particle. Therefore, instead of the previously chosen spher-
ical ice particle shape, ice particles now can be prescribed
285 as hexagonal columns or plates. The aspect ratio can be ei-
ther constant for all size bins or be changed with size fol-
lowing the approach of Mitchell (1996). Typically, with in-
creasing particle size, the deviation from an uniform aspect 335
ratio increases. In our simulations, a constant uniform aspect
ratio ($ar=1$) is used as base case. From Mitchell (1996) the
size-varying aspect ratios for plates ~~and columns are (ranging~~
290 ~~from 15 to 3000 μm with a single description) and columns~~
~~(for size ranges of 30 to 100 μm , 100 to 300 μm , and above~~
~~300 μm in diameter) are calculated from the mass-dimension 340~~
~~power laws and used for sensitivity studies.~~

295 The (relative) capacitance needed for the calculation of
deposition growth of the ice crystals is modeled using the
method of Westbrook et al. (2008) for the aspect ratios given
above. Ice crystal terminal fall velocities are calculated ac- 345
cording to Heymsfield and Westbrook (2010) using the same
300 aspect ratios.

3.2 Model initialization

3.2.1 Thermodynamics

The Asai-Kasahara model has to be initialized with vertical
profiles of temperature and dewpoint temperature either from
305 reanalysis data (here GDAS) or radiosonde profiles from
nearby stations (here Meiningen, Thuringia). Fig. 7 shows
profiles of temperature and relative humidities with respect
to liquid water and to ice, respectively, for both cases. For
case 1, profiles from both methods show a similar general
behaviour but the radiosonde profile of Meiningen measured
310 at 00 UTC is used since it provides a finer vertical resolution
than the GDAS reanalysis data ~~(cp. Fig. 7).~~ However, for 360
case 2 the Meiningen RS profile misses the humidity layer
at the level where the clouds were observed ~~and, therefore,~~
315 ~~This means that the profile is not representative for the given~~
~~meteorological situation. Therefore,~~ GDAS reanalysis data
for Leipzig at 21 UTC were chosen. Finally, both profiles 365
used show a sufficiently humid layer where the clouds were
observed, so that lifting of these layers lead to supersatura-
320 tion and subsequent cloud formation.

~~In contrast to other Asai-Kasahara model studies, updrafts~~
~~are not initialized by a heat and/or humidity pulse in certain~~
~~layers for a given period of time. Instead, As mentioned 370~~
~~above,~~ vertical velocity (updrafts and downdrafts) in the in-

ner cylinder is prescribed at cloud level ranging from h_{bot} to
 h_{top} . The center of this interval is given by $h_{mid} = (h_{top} +$
 $h_{bot})/2$ and its half-depth by $h_{depth} = (h_{top} - h_{bot})/2$. h_{bot}
ranges from 3800 m to 4100 m for case 1 and from 7000 m to
7300 m for case 2. The respective values for h_{top} are 4500 m
and 7700 m. The vertical dependency (compare Fig. 8, left)
is given by

$$f_h(h) = \frac{h_{depth}^2 - (h - h_{mid})^2}{h_{depth}^2} \quad \text{for } h_{bot} \leq h \leq h_{top} \quad (1)$$

resulting in the time- and height-dependent function

$$w(h, t) = w_{mid}(t) f_h(h) \quad \text{for } h_{bot} \leq h \leq h_{top} \quad (2)$$

and $w(h, t) = 0$ otherwise, defining $w_{mid}(t)$ as the updraft
velocity at h_{mid} . In order to match the observed wind field
distributions rather closely, $w_{mid}(t)$ is chosen as a stochastic
function

$$w_{mid}(t) = w_{ave} + f_{scal} \frac{\delta(t)^3}{|\delta(t)|} \quad (3)$$

350 where w_{ave} is the average ('large-scale') updraft velocity at
 h_{mid} varying between 0.1 m/s and 0.4 m/s, f_{scal} is the scal-
ing factor determining the range of updraft velocities (chosen
as 4 m/s to obtain a difference of minimum and maximum ve-
locity of 2 m/s), and $\delta(t)$ is a random number ranging from
-0.5 to +0.5 obtained from a linear stochastic process pro-
vided by FORTRAN. After 30 s model time a new $\delta(t)$ is
created. Different realizations of the stochastic process are
tested (see below). E.g., $w_{mid}(t)$ ranges from -0.7 m/s to
1.3 m/s if $w_{ave} = 0.3$ m/s and $f_{scal} = 4$ m/s as it is shown in
the temporal evolution and the histogram in ~~Figure Fig.~~ 8.

Due to the height dependent vertical velocity w , a horizon-
tal transport velocity u_k (exchange between inner and outer
cylinder) is induced in the Asai-Kasahara formulation for a
given model layer k .

$$u_k = - \frac{w_{k+\frac{1}{2}} \rho_{k+\frac{1}{2}} - w_{k-\frac{1}{2}} \rho_{k-\frac{1}{2}}}{f_r \Delta z \rho_k} \quad (4)$$

Full indices k indicate values at level centers whereas
half indices ($k + \frac{1}{2}$, $k - \frac{1}{2}$) describe values at level inter-
faces. $f_r = 2/r_i$ is a geometry parameter with the radius
 ~~$r_i = 1000 r_i = 100$~~ m of the inner cylinder.

The prescribed velocity field leads to the following effects
(all descriptions are related to the inner cylinder if not stated
otherwise explicitly):

- In the updraft phase: In the upper part (between h_{mid}
and h_{top}) of the updraft, mixing occurs from the inner
to the outer cylinder whereas in the lower part (between
 h_{low} and h_{mid}), horizontal transport is from the outer
cylinder into the inner one
- For downdrafts it is the other way: This means that be-
low h_{mid} drops and ice particles are transported from
the inner cylinder to the outer one and are therefore re-
moved from the inner cylinder

- below h_{low} or above h_{top} , no horizontal exchange takes place.

The question arises to which extent this dynamical behaviour reflects the real features of the observed clouds and whether this is critical for the topics aimed at in this study.

Prescribing vertical velocity in any way also means that a feedback of microphysics on dynamics due to phase changes (e.g., release of latent heat for condensing water vapor or freezing/melting processes) is not considered by the model.

3.2.2 Aerosol distribution

Since no in situ aerosol measurements are available, literature data is used. The Raman lidar observations do not show any polluted layers for both cases; therefore data from LACE98 (Petzold et al., 2002) are used which should be representative for the free troposphere over Leipzig. For case 1 values for the lower free troposphere (M6), for case 2 those from the upper free troposphere (M1) are used (see Petzold et al., 2002, Tab. 6) (see Petzold et al., 2002, Tab. 6).

4 Model results: Dynamics

In a first step, the aim is to achieve a sufficient agreement concerning macroscopic cloud features as well as (liquid phase) microphysics as far as they were observed. The following parameters describing model dynamics (updraft velocity) are varied to identify a ‘best case’ which in the second step can be used to perform sensitivity studies with respect to (ice) microphysics (see also Tables 1 and 2).

- h_{low} : ranging from 3800 m to 4100 m for the warmer and from 7000 m to 7300 m for the colder case. This parameter influences the vertical cloud extent and, therefore, liquid water content and liquid water path.
- w_{ave} : ranging from 0.1 m/s to 0.4 m/s. Higher average updraft also leads to higher LWC. Due to the lateral mixing processes the model setup requires a positive updraft velocity in average to form and maintain clouds.
- δ : Four different realizations of the stochastic process are used. This influences the timing of the cloud occurrence as well as LWC and LWP but not systematically.

All model results shown refer to the inner cylinder.

4.1 Case 1: Warm mixed-phase cloud

Figs. 9 and 11 show time-height plots of the liquid (contours, linear scale) and ice (colours, logarithmic scale) water mixing-ratio content for case 1 illustrating the cloud sensitivity with respect to variation of cloud base (h_{bot}), average vertical updraft (w_{ave}), and the realization of the stochastic

process, respectively. Liquid clouds form in the updraft regions (cp. Fig. 8) whereas in the downdrafts the liquid phase vanishes at least partly. ~~Ice forms mainly at cloudbase and immediately starts.~~ If active INP are available ice formation can take place within the liquid part of the cloud. The INP are partly already active near liquid cloud base which means that they trigger freezing as soon as the droplets are formed. Less efficient INP become active after further cooling above cloud base. After ice formation rapid depositional growth takes place and the ice particles almost immediately start to sediment. Due to the supersaturation with respect to ice even below liquid cloud base, ice particles still grow while sedimenting, reaching their maximum size before, finally, subsaturated regions are reached and ~~evaporation~~ sublimation sets in. Figs. 10 and 12 show the time evolution of liquid (lower panel) and ice water path (upper panel) for the same parameters varied, reflecting the same temporal patterns. ~~Table Tab. 1~~ summarizes the maximum values for liquid and ice water ~~mixing-ratio~~ (LWMCcontent (LWC/IWMC)), liquid and ice water path (LWP/IWP) as well as cloud droplet and ice particle number concentration (CDN/IPN) for all dynamics sensitivity runs for case 1.

One can clearly observe, that a lower h_{bot} (Fig. 9) results in a lower cloud base, larger vertical cloud extent as well as more liquid water. ~~The same trend with similar intensity~~ LWC maxima are within a factor of 2 for varying h_{bot} . A similar trend is observed for the ice phase (see also Fig. 10) 10, but IWC maxima differ only by about 25 %. However, the values of the two maxima of the condensed phase after about 15–20 min and about 40 min model time are quite different. The first maximum is more pronounced for the ice phase whereas the second one is larger for the liquid phase. While the liquid phase is dominated by the updraft velocity (see Fig. 8) the ice phase additionally depends on ~~IN~~ INP supply. In the first ice formation event at 15 min, all ~~IN~~ INP active at the current temperature actually form ice leading to an ~~IN-IPN~~ INP depletion. Due to the horizontal exchange with the outer cylinder the ~~IN-IPN~~ INP reservoir is refilled, but only to a certain extent when the second cloud event after 40 min sets in. Due to the limited ~~IN-IPN~~ INP supply the second ice maximum is weaker than the first one. The stochastic velocity fluctuations cause fluctuations in relative humidity, which are directly reflected by the liquid phase parameters whereas the ice phase generally reacts much slower. Sensitivity of CDN and IPN with respect to change of h_{bot} does not seem to be systematic.

Increasing the average updraft velocity w_{ave} leads to a similar increase of liquid water and ice as lowering h_{bot} (see Figs. 11, upper panel and 12, left). This can be expected since more water vapor flows through the cloud and is able to condense. However, a certain limit seems to be reached for W_w04, since the increase of LWP slows down (see maximum value at 40 min in Fig. 12, left). This is due to the enhanced horizontal exchanged following eq. (4). Additionally, the stronger updrafts allow the ice particles a longer presence

time in the vicinity of the cloud and, therefore, an enhanced growth at comparably high supersaturation with respect to ice before sedimentation sets in at larger sizes. This also leads to an accumulation of ice particles and, therefore, to a higher IPN. Surprisingly, CDN ~~only depends~~ depends only weakly and not systematically on w_{ave} which is in contrast to the typical enhancement of CDN with increasing updraft velocities.

Figs. 11 (lower panel) and 12 (right) show that different realizations of the stochastic process (as explained above in section 3.2.1) lead to different temporal cloud evolutions. However, differences in maximum LWP and ~~LWLR-LWC~~ LWLR-LWC are much smaller than those discussed above. Variations in maximum IWP and ~~IWLR-IWC~~ IWLR-IWC as well as CDN and IPN are in the range of about 30%. This is also true for average LWP ranging from 18 g/m² for W_r1 to 26 g/m² for W_r3. However, despite the different maxima and temporal evolutions of IWP, average IWP is almost identical for the different stochastic realizations (0.023 g/m²). This shows that changing the stochastic realization influences cloud evolution in detail (timing) but does not change the overall picture.

With maximum values between 17 and 57 g/m² the modeled liquid water path is in the same range as the observed values (20–50 g/m²), especially for the 'wetter' runs (smaller h_{bot} , larger w_{ave}). Average LWP typically is about half (40–60%) of the maximum value for most of the runs which also fits well into the observations. Ice forms within the liquid layer and sediments to about 3800 m for most runs which is less than for the observations. The (maximum) modeled ice mixing ratio is in the same order of magnitude as the observed one (about 10⁻⁷ kg/m³). The same holds for the ice water path with values of about 0.01 g/m² for both, model and observation. For the other values, no observational data is available for comparison.

4.2 Case 2: Colder mixed-phase cloud

Due to the ~~colder-lower~~ colder-lower temperatures of case 2 much more ~~INP are active and much more~~ ice is produced than in case 1 (see Figs. 13–16 as well as Tab. 2). ~~Therefore This also means that near cloud base much more active INP are available and that a further cooling within the clouds only slightly increases the number of active INP leading again to a preferential ice nucleation near liquid cloud base. Due to the lower temperatures and the more massive ice formation,~~ the virgae reach down to more than 1500 m below liquid cloud base which is in concordance with the observations. The principal behaviour with respect to the sensitivity parameters is similar as in case 1: The liquid phase is enhanced by either decreasing h_{bot} or increasing w_{ave} , showing the 'saturation' effect slightly more pronounced as in case 1. Different stochastic realizations only weakly influence the maximum and average values of the liquid phase but change the timing of occurrence. Generally, the variability of the ice phase is weaker than in case 1. The different stochastic realizations

show the highest variability in ~~IWLR-IWC~~ IWLR-IWC and IWP. Different variations of h_{bot} show almost identical IWPs, whereas changing w_{ave} at least slightly influences maximum ~~IWLR-IWC~~ IWLR-IWC and IWP, which again can be attributed to the ice particle accumulation in the updraft. Liquid water path is smaller than in case 1 and reaches maximum values between 10 and 43 g/m² which well covers the observed maximum value of about 20 g/m². Cloudnet observations show an IWC of 10⁻⁷ – 10⁻⁵ kg/m³ which is an increase by a factor of 10–100 compared to case 1. Similar values are obtained by the model results underlining the strong temperature dependency of the ice nucleation process.

5 Sensitivity studies

In the previous section it could be shown that dynamical parameters can be chosen in a way that the model results (in terms of LWP, IWP as well as cloud geometry) are in good agreement with the observations. This allows to perform sensitivity studies with respect to cloud microphysics. To cover the proper sensitivities we have to answer the question which microphysical parameters are expected to have a large influence on mixed phase microphysics and are rather uncertain to be estimated. This leads to (temperature-dependent) ~~IN number~~ IN number (N_{INP}) which directly influences ice particle number but mostly is poorly known. To be consistent with the freezing parameterization of the model, ~~N_{INP}~~ N_{INP} is varied by changing $N_{AP,r>250nm}$ which additionally is easier to observe in most cases. A second parameter is the shape of the ice particles which does not influence the primary freezing process but the subsequent growth by water vapor deposition onto existing ice particles and, therefore, the total ice mass produced. Their relative importance shall be quantified and also be compared to the influence of dynamics discussed above.

5.1 ~~IN-INP~~ IN-INP number

Changing $N_{AP,r>250nm}$ leads to a temperature-dependent change of ~~IN-INP~~ IN-INP number which is relatively small for warmer conditions. However, the effect increases with decreasing temperature. This is illustrated by the following numbers. The parameterization of DeMott et al. (2010) gives about 0.009 active ~~IN-INP~~ IN-INP per liter at standard conditions (~~N_{INP}~~ N_{INP}) when $N_{AP,r>250nm} = 10^5$ kg⁻¹ at $T = -5^\circ\text{C}$. A tenfold increase to $N_{AP,r>250nm} = 10^6$ kg⁻¹ results in about 0.012 active ~~IN-INP~~ IN-INP per liter which is a rise of only about 35%. For $T = -7^\circ\text{C}$, ~~IN-INP~~ IN-INP number rises by about 65% for a tenfold increase of $N_{AP,r>250nm}$. This shows that for those rather ~~warm-high~~ warm-high temperatures considered for case 1, a massive change in $N_{AP,r>250nm}$ leads to relatively small changes in ~~N_{INP}~~ N_{INP} and only a small effect on the ice phase can be expected. This is confirmed by Fig. 17 (left) showing liquid and ice water ~~mixing ratios~~ mixing ratios

575 [contents](#) for W_in6. Ice-mass-IWC is enhanced by less than 60 % for W_in6 and by about 160 % for W_in7 which is consistent for the given temperature range (see Tab. 3). Similar values are obtained for the change in IPN. This directly leads to the conclusion that the individual ice particles grow independently from each other. Their individual growth history is (in contrast to drop growth) only influenced by thermodynamics as long as their number is low enough which seems to be the case here.

585 This is confirmed by Fig. 18 showing drop and ice particle size distributions at the time when the maximum IWP is reached (16 min for case 1, 17 min for case 2). For case 1 (upper panel), the liquid phase (contours) is unaffected by the IN-INP enhancement. Despite the increase of ice particle number and mass the shape of the ice particle size distribution (colors) is not changed. The smallest ice particles can be observed at three discrete height (and temperature) levels caused by the temperature resolved parameterization of the potential IN-INP described in section 3.1.1. In reality this part of the spectrum showing rather freshly nucleated and fast growing ice particles should be continuous over the height range from about 4100 m to 4400 m. Nevertheless, the total number of ice particles formed is described correctly.

595 One can conclude that increasing IN-INP number therefore increases ice particle number as well as ice mass proportionally. Generally, the ice mass remains small and the liquid phase is not affected by the ice mass increase. Those results are supported by Fig. 19 (left) showing an unchanged LWP and a proportionally growing IWP for increased IN-INP numbers.

605 For the colder case 2 the parameters are varied in the same way. However, one big difference is that a tenfold increase of $N_{AP,r>250nm}$ at $T = -25^\circ\text{C}$ results in a much larger change in active IN-INP. Their number rises by 300 % from about 0.5 per liter to about 2 per liter following the parameterization. This is reflected by the IPN values in [Table Tab. 4](#). Fig. 17 (right) and [Table Tab. 4](#) show that ice mass increases in such a way that liquid water is depleted partially (C_in6 by about 50 %) or almost totally (C_in7) due to the Bergeron-Findeisen-Wegener-Bergeron-Findeisen process. Compared to C_base, ice is enhanced by a factor of 3–4 for C_in6 and about 10 for C_in7 whereas IPN increases by a factor of 12. This can also be seen in the IWP (Fig. 19, right, red lines) showing a limited increase for C_in7, especially for the first maximum after 17 min. This means that the results for C_in6 are still consistent with an independent growth of the individual ice particles (as described above) despite the relatively high ice occurrence.

620 This is verified by the size distributions in Fig. 18 (lower panel). As in case 1 the ice particle size distributions only differ by the number/mass, but not by shape. Additionally, the decrease in the liquid phase is reflected also in the drop spectrum showing a more shallow liquid part of cloud as well as droplet distribution shifted to smaller sizes.

However, for C_in7 the ice particles compete for water vapor which becomes clear from (i) the depletion of liquid water (resulting in a lower supersaturation with respect to ice) and (ii) the ice mass enhancement factor being below the value expected from the ice nucleation parameterization and below that of IPN. This means that despite the higher number of IN-INP and, therefore, ice particles, the amount of ice is limited by the thermodynamic conditions which results in the production of more but smaller ice particles, similar to the Twomey effect for drop activation.

As mentioned earlier, ice particle growth is not restricted to the liquid part of the cloud but also occurs in the layer below liquid cloud base, which is still supersaturated with respect to ice. This leads to a decrease in relative humidity in this part of the cloud, which in turn weakens or suppresses droplet formation by shifting liquid cloud base to higher altitudes. The lower LWC for the runs with higher IWC therefore cannot only be attributed to the WBF processes but also to this indirect effect.

5.2 Ice particle shape

As discussed previously, for most of the cases (except for C_in7) changing the parameters in the section above does neither influence the ice particles themselves nor their individual growth. Additionally, due to their low number, there is almost no competition of the ice particles for water vapor, and, therefore, ice water content scales linearly with ice particle number. In contrast to this, changing the ice particle shape from quasi-spherical ($ar=1$) to columns or plates with size-dependent axis ratios deviating from unity results in an increase of water vapor deposition on the individual ice particles leading to enhanced ice water content due to larger individual particles when ice particle numbers remain unchanged. This is due to (i) enhanced relative capacitance resulting in faster water vapor deposition and (ii) lower terminal velocities of the ice particles leading to longer residence times in vicinity of conditions with supersaturation with respect to ice.

Fig. 20 (left) shows the results for the runs using hexagonal columns (W_col) as prescribed ice particle type. Compared to the previous results (W_base, W_in6, W_in7) more ice mass is produced (see [Table Tab. 3](#)) but still the liquid part of the cloud remains unaffected (compare also LWP and IWP in Fig. 19, left). Similar results are obtained for the assumption of plate-like ice particles (W_pla). The mass increase results from the larger ice particle size due to the reasons discussed above which can be seen from Fig. 21 showing the size distributions for W_col at different times. On the upper left panel W_col is shown after 16 min corresponding to Fig. 18. Compared to W_base, larger ice particles are produced leading to more ice mass (equivalent radius up to $300\ \mu\text{m}$ compared to $189\text{--}238\ \mu\text{m}$ for the base case). Additionally, due to the lower fall speed of the columns ($1.03\ \text{m/s}$ vs. $1.75\text{--}2.24\ \text{m/s}$), the maximum of the ice is at about 4200 m compared to 4100 m

for the base case. On the upper right panel, size distributions after 21 min are shown corresponding to the IWP maximum of W_col. Ice particles have grown larger (equivalent radius up to $378 \mu\text{m}$, length of the columns increases from about 3 mm to 4.5 mm) and sedimentation has developed further with increasing terminal velocity (1.13 m/s). Similar results are obtained for plates (W_pla) with terminal velocities of 0.89–1.21 m/s, equivalent radii of 300–476 μm and maximum dimension of 1.8–3.2 mm.

The lower terminal velocity of columns and plates despite their larger size is leading to the stronger tilting of the virgae. Additionally, ice particle number IPN is enhanced by about 30% although ice nucleation is identical to W_base. This can be attributed to the lower fall velocities, too, leading to an accumulation of ice particles. The differences between W_col and W_pla are caused by both, the higher relative capacitances of and lower terminal fall velocities of plates compared to columns (at least when their axis ratios are chosen following Mitchell (1996)).

For case 2 (C_col and C_pla), the liquid water reduction due to the Bergeron-Findeisen process is similar to C_in6 (see Fig. 20, right, and Table Tab. 4). In contrast to the respective case 1 runs, less ice is produced than for C_in7. The tilting of the virgae is not as strong as in W_col which is due to the larger ice particle sizes leading to higher terminal fall velocities (1.43–1.60 m/s). Additionally, the lower air density leads to an increase of terminal velocity of more than 10% independently from shape. Fig. 21 (lower panels) show panel shows the size distributions for C_col at different times. Due to the longer growth time larger individual ice particles than in case 1 are produced (equivalent radius up to 600 μm compared to 300 μm for the base case).

To decide whether independent ice particle growth or competition occurs, further runs with less IN-INP (C_col_in4 and C_pla_in4) are discussed (see Fig. 19, right). IWMR-IWC and IWP of these runs (in4) are about one third of the values of the respective runs with more IN-INP (in5). For ice particle number, a factor of slightly more than three occurs which means that a weak competition for water vapor occurs for C_col and C_pla resulting in slightly smaller individual ice particles compared to C_col_in4 and C_pla_in4.

6 Conclusions

The model system AK-SPECS was applied to simulate dynamical and microphysical processes within altocumulus clouds. Sensitivity studies on relative contributions on cloud evolution as well as comparisons to observations were made.

Variation of the dynamic parameters as it was done in section 4 leads to systematic differences mainly in the liquid phase (LWMRLWC, LWP) which can easily be explained. More liquid water is produced when either cloud base is lowered (corresponding to a larger vertical cloud extent) or vertical wind velocity is increased. However, the effects of

the dynamics on the ice phase are surprisingly small, at least smaller than those on the liquid phase. Increasing vertical velocity leads to an accumulation of the smaller ice particles in the enhanced updraft.

On the other hand, much larger differences in terms of IWMR-IWC and IWP were found when microphysical parameters like IN-INP number or ice particle shape were varied under identical dynamic conditions. This is valid for both cases studied. However, at least for the ice nucleation parameterization used, sensitivity of IN-INP number strongly increased with decreasing temperature.

This means that relatively large differences concerning the ice phase can only be reached when either IN-INP number differs considerably or ice particle shape is different (which should not be the case for relatively similar thermodynamical conditions). After Fukuta and Takahashi (1999) for case 1 with temperatures of about -6°C column-like ice particles with $ar = 0.1$ could be expected (corresponding to W_col) whereas for case 2 ($T < -24^\circ\text{C}$) hexagonal particles with $ar = 1$ are most likely (e.g., C_base). Those ice shapes were observed in laboratory studies at water saturation which was also valid for the observed cases when ice formed by immersion freezing within the liquid layer of the cloud. However, below liquid cloud base supersaturation with respect to ice decreases. These ice shapes can also explain why a depletion of the liquid phase was not observed in case 2 as it was predicted by the sensitivity studies using either columns or plates as prescribed shape. Generally, the liquid phase is affected considerably only when enough ice particles are present which typically is the case for cold conditions with a sufficient amount of IN-INP and fast growing ice particle shapes (most effective for large deviations from spherical shapes).

Acknowledgements. Funding—This study was supported by the Deutsche Forschungsgemeinschaft DFG-project UDINE-

urlstyle

Althausen, D., Engelmann, R., Baars, H., Heese, B., Ansmann, A., Müller, D., and Komppula, M.: Portable Raman Lidar PollyXT for Automated Profiling of Aerosol Backscatter, Extinction, and Depolarization, *J. Atmos. Oceanic Technol.*, 26, 2366–2378, 2009.

Asai, T. and Kasahara, A.: A theoretical study of compensating downward motions associated with cumulus clouds, *JOURNAL OF THE ATMOSPHERIC SCIENCES*, 24, 487–496, 1967.

Bauer-Pfundstein, M. R. and Grsdorf, U.: Target Separation and Classification Using Cloud Radar Doppler Spectra, in: *Proceedings of the 33rd Conference on Radar Meteorology, 2007.*

Buehl, J., Ansmann, A., Seifert, P., Baars, H., and Engelmann, R.: Toward a quantitative characterization of heterogeneous ice formation with lidar (DFG) under Grant AN 258/radar: Comparison of CALIPSO/CloudSat with ground-based observations,

- GEOPHYSICAL RESEARCH LETTERS, 40, 4404–4408, 2013.
- Bühl, J., Engelmann, R., and Ansmann, A.: Removing the Laser-Chirp Influence from Coherent Doppler Lidar Datasets by Two-Dimensional Deconvolution, *J. Atmos. Oceanic Technol.*, 29, 1042–1051, 2012.
- Dearden, C., Connolly, P. J., Choulaton, T., Field, P. R., and Heymsfield, A. J.: Factors influencing ice formation and growth in simulations of a mixed-phase wave cloud, *JOURNAL OF ADVANCES IN MODELING EARTH SYSTEMS*, 4, 2012.
- DeMott, P. J., Prenni, A. J., Liu, X., Kreidenweis, S. M., Petters, M. D., Twohy, C. H., Richardson, M. S., Eidhammer, T., and Rogers, D. C.: Predicting global atmospheric ice nuclei distributions and their impacts on climate, *PROCEEDINGS OF THE NATIONAL ACADEMY OF SCIENCES OF THE UNITED STATES OF AMERICA*, 107, 11217–11222, 2010.
- Diehl, K., Simmel, M., and Würzler, S.: Numerical sensitivity studies on the impact of aerosol properties and drop freezing modes on the glaciation, microphysics, and dynamics of clouds, *JOURNAL OF GEOPHYSICAL RESEARCH-ATMOSPHERES*, 111, 2006.
- Eidhammer, T., DeMott, P. J., Prenni, A. J., Petters, M. D., Twohy, C. H., Rogers, D. C., Stith, J., Heymsfield, A., Wang, Z., Pratt, K. A., Prather, K. A., Murphy, S. M., Seinfeld, J. H., Subramanian, R., and Kreidenweis, S. M.: Ice Initiation by Aerosol Particles: Measured and Predicted Ice Nuclei Concentrations versus Measured Ice Crystal Concentrations in an Orographic Wave Cloud, *JOURNAL OF THE ATMOSPHERIC SCIENCES*, 67, 2417–2436, 2010.
- Field, P. R., Heymsfield, A. J., Shipway, B. J., DeMott, P. J., Pratt, K. A., Rogers, D. C., Stith, J., and Prather, K. A.: Ice in Clouds Experiment Layer Clouds. Part II: Testing Characteristics of Heterogeneous Ice Formation in Lee-Wave Clouds, *JOURNAL OF THE ATMOSPHERIC SCIENCES*, 69, 1066–1079, 2012.
- Fridlind, A. M., Aekerman, A. S., McFarquhar, G., Zhang, G., Poellot, M. R., DeMott, P. J., Prenni, A. J., and Heymsfield, A. J.: Ice properties of single-layer stratocumulus during the Mixed-Phase Arctic Cloud Experiment: 2. Model results, *JOURNAL OF GEOPHYSICAL RESEARCH-ATMOSPHERES*, 112, 2007.
- Fukuta, N. and Takahashi, T.: The Growth of Atmospheric Ice Crystals: A Summary of Findings in Vertical Supercooled Cloud Tunnel Studies, *JOURNAL OF THE ATMOSPHERIC SCIENCES*, 56, 1963–1979, 1999.
- Hartmann, S., Augustin, S., Clauss, T., Wex, H., Santl-Temkiv, T., Voigtlander, J., Niedermeier, D., and Stratmann, F.: Immersion freezing of ice nucleation active protein complexes, *Atmospheric Chemistry and Physics*, 13, 5751–5766, 2013.
- Heymsfield, A. J. and Westbrook, C. D.: Advances in the Estimation of Ice Particle Fall Speeds Using Laboratory and Field Measurements, *JOURNAL OF THE ATMOSPHERIC SCIENCES*, 67, 2469–2482, 2010.
- Hogan, R. J., Mittermaier, M. P., and Illingworth, A. J.: The Retrieval of Ice Water Content from Radar Reflectivity Factor and Temperature and Its Use in Evaluating a Mesoscale Model, *J. Appl. Meteor. Climatol.*, 45, 301–317, 2006.
- Illingworth, A. J., Hogan, R. J., O'Connor, E. J., Bouniol, D., Delanoë, J., Pelon, J., Protat, A., Brooks, M. E., Gaussiat, N., Wilson, D. R., Donovan, D. P., Baltink, H. K., van Zadelhoff, G. J., Eastment, J. D., Goddard, J. W. F., Wrench, C. L., Haefelin, M., Krasnov, O. A., Russechenberg, H. W. J., Piriou, J.-M., Vinit, F., Seifert, A., Tompkins, A. M., and Willén, U.: Cloudnet, *Bull. Amer. Meteor. Soc.*, 88, 883–898, 2007.
- Meyers, M., DeMott, P., and Cotton, W.: NEW PRIMARY ICE-NUCLEATION PARAMETERIZATIONS IN AN EXPLICIT CLOUD MODEL, *JOURNAL OF APPLIED METEOROLOGY*, 31, 708–721, 1992.
- Mitchell, D.: Use of mass-15. We also acknowledge funding from the EU FP7-ENV-2013 programme “impact of Biogenic vs. Anthropogenic emissions on Clouds and area-dimensional power laws for determining precipitation particle terminal velocities Climate: towards a Holistic UnderStanding” (BACCHUS), *JOURNAL OF THE ATMOSPHERIC SCIENCES*, 53, 1710–1723, 1996. project.no.603445.
- Murray, B. J., O'Sullivan, D., Atkinson, J. D., and Webb, M. E.: Ice nucleation by particles immersed in supercooled cloud droplets, *Chem. Soc. Rev.*, 41, 6519–6554, 2012.
- O'Sullivan, D., Murray, B. J., Malkin, T. L., Whale, T. F., Umo, N. S., Atkinson, J. D., Price, H. C., Baustian, K. J., Browse, J., and Webb, M. E.: Ice nucleation by fertile soil dusts: relative importance of mineral and biogenic components, *Atmospheric Chemistry and Physics*, 14, 1853–1867, 2014.

References

- Althausen, D., Engelmann, R., Baars, H., Heese, B., Ansmann, A., Müller, D., and Komppula, M.: Portable Raman Lidar PollyXT for Automated Profiling of Aerosol Backscatter, Extinction, and Depolarization, *J. Atmos. Oceanic Technol.*, 26, 2366–2378, doi:10.1175/2009JTECHA1304.1, 2009.
- Asai, T. and Kasahara, A.: A theoretical study of compensating downward motions associated with cumulus clouds, *JOURNAL OF THE ATMOSPHERIC SCIENCES*, 24, 487–496, doi:10.1175/1520-0469(1967)024<0487:ATSOTC>2.0.CO;2, 1967.
- Bauer-Pfundstein, M. R. and Görsdorf, U.: Target Separation and Classification Using Cloud Radar Doppler-Spectra, in: Proceedings of the 33rd Conference on Radar Meteorology, 2007.
- Bergeron, T.: On the physics of clouds and precipitation, in: *Process verbaux de l'association de Meteorologie*, pp. 156–178, International Union of Geodesy and Geophysics, Lisboa, Portugal, 1935.
- Buehl, J., Ansmann, A., Seifert, P., Baars, H., and Engelmann, R.: Toward a quantitative characterization of heterogeneous ice formation with lidar/radar: Comparison of CALIPSO/CloudSat with ground-based observations, *GEOPHYSICAL RESEARCH LETTERS*, 40, 4404–4408, doi:10.1002/grl.50792, 2013.
- Bühl, J., Engelmann, R., and Ansmann, A.: Removing the Laser-Chirp Influence from Coherent Doppler Lidar Datasets by Two-Dimensional Deconvolution, *J. Atmos. Oceanic Technol.*, 29, 1042–1051, doi:10.1175/JTECH-D-11-00144.1, 2012.
- Carey, L. D., Niu, J., Yang, P., Kankiewicz, J. A., Larson, V. E., and Vonder Haar, T. H.: The Vertical Profile of Liquid and Ice

- Water Content in Midlatitude Mixed-Phase Altocumulus Clouds, *J. Appl. Meteorology and Climate*, 47, 2487–2495, 2008. ⁹⁵⁵
- Dearden, C., Connolly, P. J., Choullarton, T., Field, P. R., and Heymsfield, A. J.: Factors influencing ice formation and growth in simulations of a mixed-phase wave cloud, *JOURNAL OF ADVANCES IN MODELING EARTH SYSTEMS*, 4, doi:10.1029/2012MS000163, 2012. ⁹⁶⁰
- DeMott, P. J., Prenni, A. J., Liu, X., Kreidenweis, S. M., Petters, M. D., Twohy, C. H., Richardson, M. S., Eidhammer, T., and Rogers, D. C.: Predicting global atmospheric ice nuclei distributions and their impacts on climate, *PROCEEDINGS OF THE NATIONAL ACADEMY OF SCIENCES OF THE UNITED STATES OF AMERICA*, 107, 11 217–11 222, doi:10.1073/pnas.0910818107, 2010. ⁹⁶⁵
- Diehl, K., Simmel, M., and Wurzler, S.: Numerical sensitivity studies on the impact of aerosol properties and drop freezing modes on the glaciation, microphysics, and dynamics of clouds, *JOURNAL OF GEOPHYSICAL RESEARCH-ATMOSPHERES*, 111, doi:10.1029/2005JD005884, 2006. ⁹⁷⁰
- Eidhammer, T., DeMott, P. J., Prenni, A. J., Petters, M. D., Twohy, C. H., Rogers, D. C., Stith, J., Heymsfield, A., Wang, Z., Pratt, K. A., Prather, K. A., Murphy, S. M., Seinfeld, J. H., Subramanian, R., and Kreidenweis, S. M.: Ice Initiation by Aerosol Particles: Measured and Predicted Ice Nuclei Concentrations versus Measured Ice Crystal Concentrations in an Orographic Wave Cloud, *JOURNAL OF THE ATMOSPHERIC SCIENCES*, 67, 2417–2436, doi:10.1175/2010JAS3266.1, 2010. ⁹⁸⁰
- Field, P. R., Heymsfield, A. J., Shipway, B. J., DeMott, P. J., Pratt, K. A., Rogers, D. C., Stith, J., and Prather, K. A.: Ice in Clouds Experiment-Layer Clouds. Part II: Testing Characteristics of Heterogeneous Ice Formation in Lee Wave Clouds, *JOURNAL OF THE ATMOSPHERIC SCIENCES*, 69, 1066–1079, doi:10.1175/JAS-D-11-026.1, 2012. ⁹⁸⁵
- Findeisen, W.: Kolloid-meteorologische Vorgänge bei Niederschlagsbildung, *Meteorolog. Z.*, 55, 121–133, 1938. ⁹⁹⁰
- Fleishauer, R. P., Larson, V. E., and Vonder Haar, T. H.: Observed Microphysical Structure of Midlevel, Mixed-Phase Clouds, *J. Atmos. Sci.*, 59, 1779–1804, 2002.
- Fridlind, A. M., Ackerman, A. S., McFarquhar, G., Zhang, G., Poellot, M. R., DeMott, P. J., Prenni, A. J., and Heymsfield, A. J.: Ice properties of single-layer stratocumulus during the Mixed-Phase Arctic Cloud Experiment: 2. Model results, *JOURNAL OF GEOPHYSICAL RESEARCH-ATMOSPHERES*, 112, doi:10.1029/2007JD008646, 2007. ⁹⁹⁵
- Fukuta, N. and Takahashi, T.: The Growth of Atmospheric Ice Crystals: A Summary of Findings in Vertical Supercooled Cloud Tunnel Studies, *JOURNAL OF THE ATMOSPHERIC SCIENCES*, 56, 1963–1979, doi:10.1175/1520-0469(1999)056<1963:TGOAIC>2.0.CO;2, 1999. ¹⁰⁰⁰
- Hartmann, S., Augustin, S., Clauss, T., Wex, H., Santl-Temkiv, T., Voigtlander, J., Niedermeier, D., and Stratmann, F.: Immersion freezing of ice nucleation active protein complexes, *Atmospheric Chemistry and Physics*, 13, 5751–5766, doi:10.5194/acp-13-5751-2013, 2013. ¹⁰⁰⁵
- Heymsfield, A. J. and Westbrook, C. D.: Advances in the Estimation of Ice Particle Fall Speeds Using Laboratory and Field Measurements, *JOURNAL OF THE ATMOSPHERIC SCIENCES*, 67, 2469–2482, doi:10.1175/2010JAS3379.1, 2010. ¹⁰¹⁰
- Hogan, R. J., Mittermaier, M. P., and Illingworth, A. J.: The Retrieval of Ice Water Content from Radar Reflectivity Factor and Temperature and Its Use in Evaluating a Mesoscale Model, *J. Appl. Meteor. Climatol.*, 45, 301–317, doi:10.1175/JAM2340.1, 2006.
- Illingworth, A. J., Hogan, R. J., O'Connor, E. J., Bouniol, D., Delanoë, J., Pelon, J., Protat, A., Brooks, M. E., Gaussiat, N., Wilson, D. R., Donovan, D. P., Baltink, H. K., van Zadelhoff, G.-J., Eastment, J. D., Goddard, J. W. F., Wrench, C. L., Haefelin, M., Krasnov, O. A., Russchenberg, H. W. J., Piriou, J.-M., Vinit, F., Seifert, A., Tompkins, A. M., and Willén, U.: Cloudnet, *Bull. Amer. Meteor. Soc.*, 88, 883–898, doi:10.1175/JAM2340.1, 2006.
- Kanitz, T., Seifert, P., Ansmann, A., Engelmann, R., Althausen, D., Casiccia, C., and Rohwer, E. G.: Contrasting the impact of aerosols at northern and southern midlatitudes on heterogeneous ice formation, *Geophysical Res. Letters*, 38, L17 802, {doi:10.1029/2011GL048532}, 2011.
- Korolev, A. and Field, P. R.: The Effect of Dynamics on Mixed-Phase Clouds: Theoretical Considerations, *J. Atmos. Sci.*, 65, 66–86, 2008.
- MEYERS, M., DEMOTT, P., and COTTON, W.: NEW PRIMARY ICE-NUCLEATION PARAMETERIZATIONS IN AN EXPLICIT CLOUD MODEL, *JOURNAL OF APPLIED METEOROLOGY*, 31, 708–721, doi:10.1175/1520-0450(1992)031<0708:NPINPI>2.0.CO;2, 1992.
- Mitchell, D.: Use of mass- and area-dimensional power laws for determining precipitation particle terminal velocities, *JOURNAL OF THE ATMOSPHERIC SCIENCES*, 53, 1710–1723, doi:10.1175/1520-0469(1996)053<1710:UOMAAD>2.0.CO;2, 1996.
- Murray, B. J., O'Sullivan, D., Atkinson, J. D., and Webb, M. E.: Ice nucleation by particles immersed in supercooled cloud droplets, *Chem. Soc. Rev.*, 41, 6519–6554, 2012.
- O'Sullivan, D., Murray, B. J., Malkin, T. L., Whale, T. F., Umo, N. S., Atkinson, J. D., Price, H. C., Baustian, K. J., Browse, J., and Webb, M. E.: Ice nucleation by fertile soil dusts: relative importance of mineral and biogenic components, *Atmospheric Chemistry and Physics*, 14, 1853–1867, doi:10.5194/acp-14-1853-2014, 2014.
- Petzold, A., Fiebig, M., Flentje, H., Keil, A., Leiterer, U., Schroder, F., Stifter, A., Wendisch, M., and Wendling, P.: Vertical variability of aerosol properties observed at a continental site during the Lindenberg Aerosol Characterization Experiment (LACE 98), *JOURNAL OF GEOPHYSICAL RESEARCH-ATMOSPHERES*, 107, doi:10.1029/2001JD001043, 2002.
- Phillips, V. T. J., DeMott, P. J., and Andronache, C.: An empirical parameterization of heterogeneous ice nucleation for multiple chemical species of aerosol, *J. Atmos. Sci.*, 65, 2757–2783, 2008.
- Pospichal, B., Kilian, P., and Seifert, P.: Performance of cloud liquid water retrievals from ground-based remote sensing observations over Leipzig, in: *Proceedings of the 9th International Symposium on Tropospheric Profiling (ISTP)*, 2012.
- Shipway, B. J. and Hill, A. A.: Diagnosis of systematic differences between multiple parametrizations of warm rain microphysics using a kinematic framework, *Q. J. R. Meteorol. Soc.*, 138, 2196–2211, doi:10.1002/qj.1913, 2012.
- Simmel, M. and Wurzler, S.: Condensation and activation in sectional cloud microphysical models, *ATMOSPHERIC RE-*

- SEARCH, 80, 218–236, doi:10.1016/j.atmosres.2005.08.002, 2006.
- 1015 Smith, A. J., Larson, V. E., Niu, J., Kankiewicz, J. A., and Carey, L. D.: Processes that generate and deplete liquid water and snow in thin midlevel mixed-phase clouds, *J. Geophys. Res.*, 114, D12 203, doi:10.1029/2008JD011531, 2009.
- 1020 Sun, J., Ariya, P. A., Leighton, H. G., and Yau, M. K.: Modeling Study of Ice Formation in Warm-Based Precipitating Shallow Cumulus Clouds, *JOURNAL OF THE ATMOSPHERIC SCIENCES*, 69, 3315–3335, doi:10.1175/JAS-D-11-0344.1, 2012.
- 1025 Warren, S. G., Hahn, C. J., London, J., Chervin, R. M., and Jenne, R.: Global distribution of total cloud cover and cloud type amount over land, Tech. Rep. Tech. Note TN-317 STR, NCAR, 1998a.
- Warren, S. G., Hahn, C. J., London, J., Chervin, R. M., and Jenne, R.: Global distribution of total cloud cover and cloud type amount over the ocean, Tech. Rep. Tech. Note TN-317 STR, NCAR, 1998b.
- 1030 Wegener, A.: *Thermodynamik der Atmosphäre*, J. A. Barth Verlag, 1911.
- Westbrook, C. D., Hogan, R. J., and Illingworth, A. J.: The capacitance of pristine ice crystals and aggregate snowflakes, *JOURNAL OF THE ATMOSPHERIC SCIENCES*, 65, 206–219, doi:10.1175/2007JAS2315.1, 2008.
- ~~Petzold, A., Fiebig, M., Flentje, H., Keil, A., Leiterer, U., Schroder, F., Stifter, A., Wendisch, M., and Wendling, P.: Vertical variability of aerosol properties observed at a continental site during the Lindenberg Aerosol Characterization Experiment (LACE-98), *JOURNAL OF GEOPHYSICAL RESEARCH-ATMOSPHERES*, 107, , 2002.~~
- ~~Phillips, V. T. J., DeMott, P. J., and Andronache, C.: An empirical parameterization of heterogeneous ice nucleation for multiple chemical species of aerosol, *J. Atmos. Sci.*, 65, 2757–2783, 2008.~~
- ~~Pospichal, B., Kilian, P., and Seifert, P.: Performance of cloud liquid water retrievals from ground-based remote sensing observations over Leipzig, in: *Proceedings of the 9th International Symposium on Tropospheric Profiling (ISTP)*, 2012.~~
- ~~Simmel, M. and Wurzler, S.: Condensation and activation in sectional cloud microphysical models, *ATMOSPHERIC RESEARCH*, 80, 218–236, , 2006.~~
- ~~Sun, J., Ariya, P. A., Leighton, H. G., and Yau, M. K.: Modeling Study of Ice Formation in Warm-Based Precipitating Shallow Cumulus Clouds, *JOURNAL OF THE ATMOSPHERIC SCIENCES*, 69, 3315–3335, , 2012.~~
- 1060 ~~Westbrook, C. D., Hogan, R. J., and Illingworth, A. J.: The capacitance of pristine ice crystals and aggregate snowflakes, *JOURNAL OF THE ATMOSPHERIC SCIENCES*, 65, 206–219, , 2008.~~

Table 1. Overview of the model results for the dynamic sensitivity runs for the warmer case 1 (maximum values of L/FWMR/IWC: liquid/ice water mixing-ratio/content, L/IWP: liquid/ice water path, CDN: cloud drop number, IPN: Ice particle number).

run	parameter value differing from base case	<u>LW</u> <u>MR</u> - <u>LWC</u> g/kg·m ³	<u>F</u> <u>W</u> <u>MR</u> - <u>IWC</u> 10 ⁻³ g/kg·m ³	LWP g/m ²	IWP 10 ⁻³ g/m ²	CDN cm ⁻³	IPN l ⁻¹
W_base	—	<u>0.277</u> - <u>0.355</u>	<u>0.304</u> - <u>0.379</u>	41.33	62.27	46.89	0.0197
W_h38	$h_{bot} = 3800$ m	<u>0.332</u> - <u>0.426</u>	<u>0.329</u> - <u>0.408</u>	57.05	73.11	48.63	0.0235
W_h40	$h_{bot} = 4000$ m	<u>0.225</u> - <u>0.289</u>	<u>0.286</u> - <u>0.357</u>	28.58	58.12	61.48	0.0240
W_h41	$h_{bot} = 4100$ m	<u>0.170</u> - <u>0.219</u>	<u>0.259</u> - <u>0.324</u>	18.23	45.81	59.53	0.0208
W_w01	$w_{ave} = 0.1$ m/s	<u>0.147</u> - <u>0.187</u>	<u>0.160</u> - <u>0.200</u>	17.41	31.73	43.36	0.0138
W_w02	$w_{ave} = 0.2$ m/s	<u>0.232</u> - <u>0.297</u>	<u>0.241</u> - <u>0.300</u>	32.86	47.18	54.57	0.0175
W_w04	$w_{ave} = 0.4$ m/s	<u>0.297</u> - <u>0.382</u>	<u>0.359</u> - <u>0.448</u>	44.48	78.25	52.66	0.0219
W_r1	stoch. realiz. r1	<u>0.261</u> - <u>0.336</u>	<u>0.254</u> - <u>0.316</u>	40.32	54.85	64.26	0.0163
W_r3	stoch. realiz. r3	<u>0.296</u> - <u>0.381</u>	<u>0.252</u> - <u>0.314</u>	42.88	54.48	43.03	0.0167
W_r4	stoch. realiz. r4	<u>0.269</u> - <u>0.346</u>	<u>0.197</u> - <u>0.245</u>	40.91	46.93	47.42	0.0151

Table 2. Overview of the model results for the dynamic sensitivity runs for the colder case 2 (maximum values of L/FWMR/IWC: liquid/ice water mixing-ratio/content, L/IWP: liquid/ice water path, CDN: cloud drop number, IPN: Ice particle number).

run	parameter value differing from base case	<u>LW</u> <u>MR</u> - <u>LWC</u> g/kg·m ³	<u>F</u> <u>W</u> <u>MR</u> - <u>IWC</u> g/kg·m ³	LWP g/m ²	IWP g/m ²	CDN cm ⁻³	IPN l ⁻¹
C_base	—	<u>0.215</u> - <u>0.377</u>	<u>0.026</u> - <u>0.041</u>	29.35	10.71	70.56	0.462
C_h70	$h_{bot} = 7000$ m	<u>0.258</u> - <u>0.452</u>	<u>0.030</u> - <u>0.048</u>	43.06	11.34	71.33	0.432
C_h72	$h_{bot} = 7200$ m	<u>0.169</u> - <u>0.296</u>	<u>0.022</u> - <u>0.035</u>	18.71	10.11	90.51	0.396
C_h73	$h_{bot} = 7300$ m	<u>0.122</u> - <u>0.215</u>	<u>0.018</u> - <u>0.028</u>	10.54	9.27	77.61	0.337
C_w01	$w_{ave} = 0.1$ m/s	<u>0.126</u> - <u>0.219</u>	<u>0.025</u> - <u>0.040</u>	17.19	8.01	76.98	0.292
C_w02	$w_{ave} = 0.2$ m/s	<u>0.181</u> - <u>0.316</u>	<u>0.027</u> - <u>0.044</u>	25.89	9.42	74.40	0.415
C_w04	$w_{ave} = 0.4$ m/s	<u>0.229</u> - <u>0.402</u>	<u>0.028</u> - <u>0.045</u>	30.58	11.85	98.37	0.439
C_r1	stoch. realiz. r1	<u>0.209</u> - <u>0.366</u>	<u>0.014</u> - <u>0.023</u>	29.37	6.57	86.64	0.257
C_r3	stoch. realiz. r3	<u>0.228</u> - <u>0.399</u>	<u>0.029</u> - <u>0.046</u>	30.22	9.95	79.65	0.341
C_r4	stoch. realiz. r4	<u>0.213</u> - <u>0.373</u>	<u>0.031</u> - <u>0.049</u>	29.53	8.33	95.89	0.419

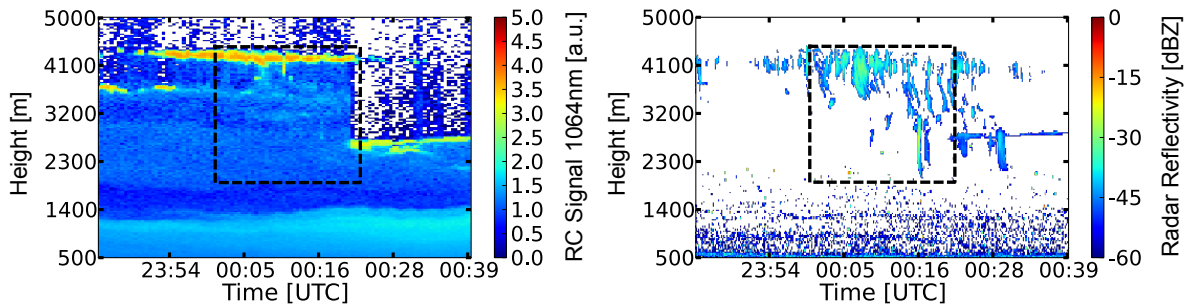


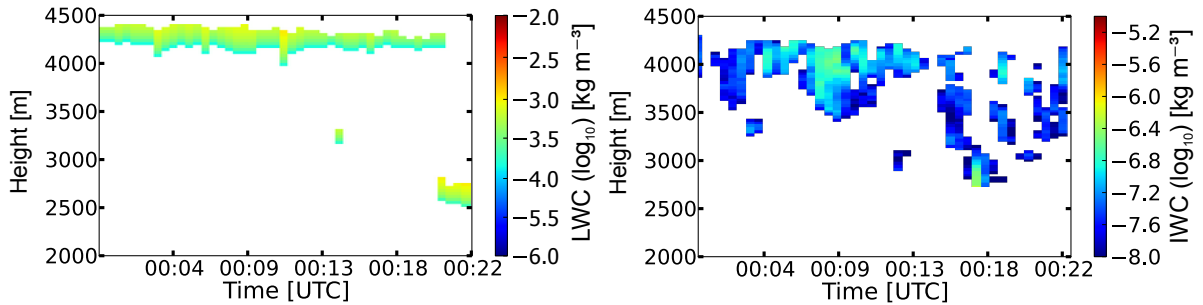
Fig. 1. Lidar and radar observations on 17 September 2011 (case 1). Left: Lidar range-corrected 1064 nm signal (in logarithmic scale, arbitrary units a. u.), right: radar reflectivity. The dashed box denotes the region for which case 1 observations are shown in the following figures.

Table 3. Overview of the model results for the microphysical sensitivity runs for the warmer case 1 (maximum values of L/IWMIWC: liquid/ice water [mixing-ratiocontent](#), L/IWP: liquid/ice water path, CDN: cloud drop number, IPN: Ice particle number).

run	parameter value differing from base case	LWMIWC g/kg-m ³	IWMIWC 10 ⁻³ g/kg-m ³	LWP g/m ²	IWP g/m ²	CDN cm ⁻³	IPN l ⁻¹
W_in6	$N_{AP,r>250nm} = 10^6 \text{ kg}^{-1}$	0.276-0.354	0.496-0.619	41.31	0.10	46.69	0.0296
W_in7	$N_{AP,r>250nm} = 10^7 \text{ kg}^{-1}$	0.276-0.354	0.801-1.000	41.24	0.17	41.61	0.0450
W_col	ice shape: columns	0.275-0.353	1.467-1.830	41.20	0.27	42.90	0.0257
W_pla	ice shape: plates	0.275-0.353	2.285-2.850	41.13	0.45	43.41	0.0267

Table 4. Overview of the model results for the microphysical sensitivity runs for the colder case 2 (maximum values of L/IWMIWC: liquid/ice water [mixing-ratiocontent](#), L/IWP: liquid/ice water path, CDN: cloud drop number, IPN: Ice particle number).

run	parameter value differing from base case	LWMIWC g/kg-m ³	IWMIWC g/kg-m ³	LWP g/m ²	IWP g/m ²	CDN cm ⁻³	IPN l ⁻¹
C_in6	$N_{AP,r>250nm} = 10^6 \text{ kg}^{-1}$	0.128-0.224	0.089-0.140	13.09	34.75	80.29	1.380
C_in7	$N_{AP,r>250nm} = 10^7 \text{ kg}^{-1}$	0.021-0.036	0.265-0.446	2.58	57.98	46.67	5.208
C_col	ice shape: columns	0.135-0.237	0.139-0.223	14.33	46.78	78.40	0.462
C_col.in4	ice shape: columns, $N_{AP,r>250nm} = 10^4 \text{ kg}^{-1}$	0.216-0.378	0.048-0.076	30.01	14.93	74.75	0.139
C_pla	ice shape: plates	0.104-0.182	0.183-0.294	9.94	57.11	39.41	0.472
C_pla.in4	ice shape: plates, $N_{AP,r>250nm} = 10^4 \text{ kg}^{-1}$	0.207-0.362	0.064-0.102	27.80	19.21	74.44	0.129

**Fig. 2.** Lidar observations on 17 September 2011 (Cloudnet derived water contents for case 1). Left: [Ice-Liquid](#) water content/IWC, right: [range-corrected-1064 nm-signal-ice water content](#) (both in logarithmic scale, arbitrary units a. u.).

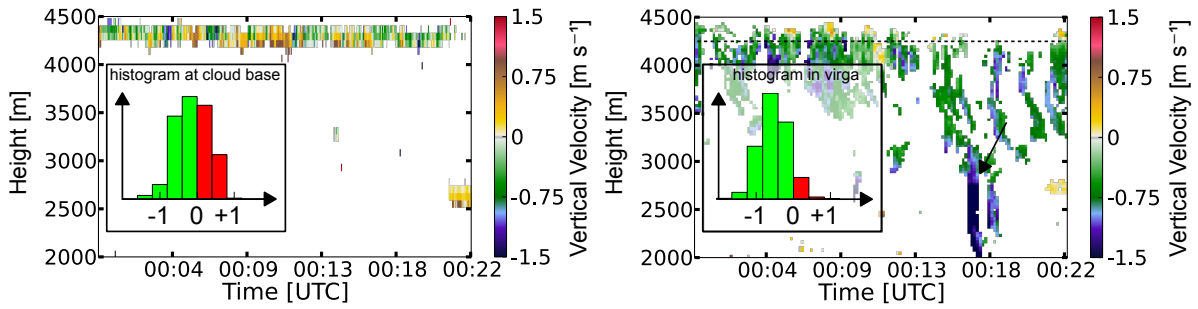


Fig. 3. Vertical velocity for case 1. Left: derived from radar-observations-lidar (valid for large-particles; virga more numerous smaller droplets at cloud base), right: derived from lidar-radar observations (valid for more numerous smaller droplets at cloud base large particles; virgae).

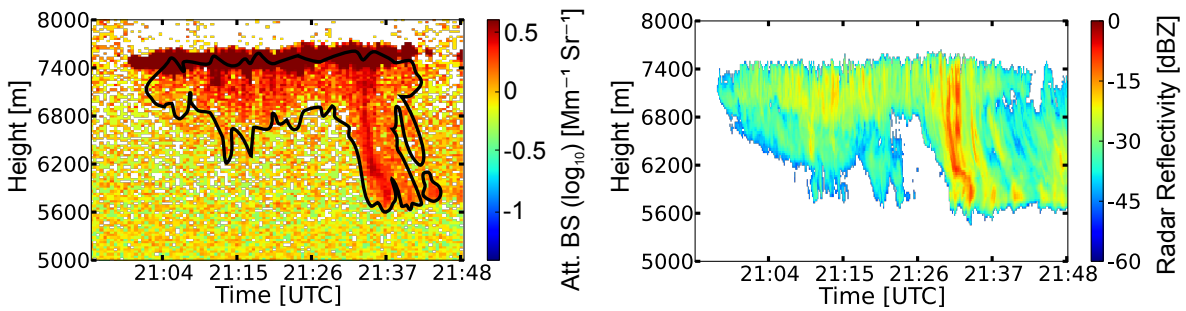


Fig. 4. Lidar and radar observations on 2 August 2012 (case 2). Left: Ice-water content IWC, right: 1064-532 nm attenuated backscatter coefficient, right: radar reflectivity.

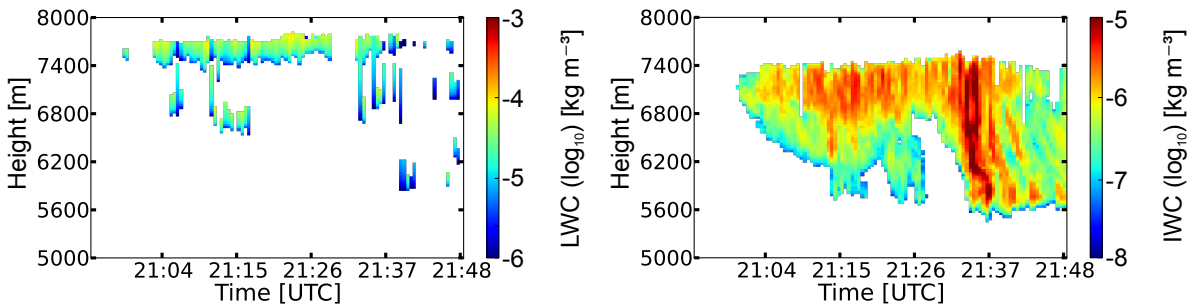


Fig. 5. Vertical velocity-Cloudnet derived water contents for case 22. Left: Liquid water content, derived from radar observations right: ice water content (both in logarithmic scale).

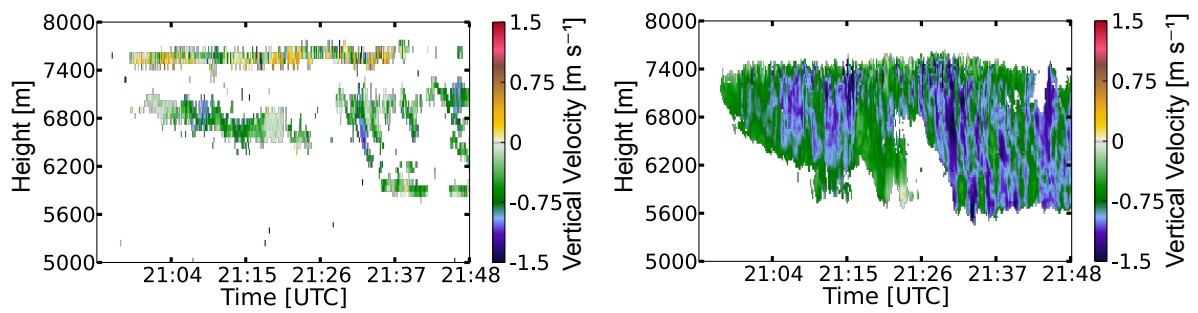


Fig. 6. Vertical velocity for case 2. Left: derived from lidar (valid for more numerous smaller droplets at cloud base), right: derived from radar observations (valid for large particles; virgae).

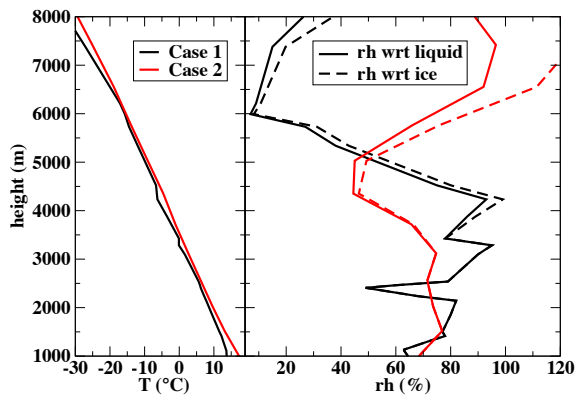


Fig. 7. Vertical profiles of temperature (left) and relative humidity (right) with respect to liquid water (full lines) and ice (dashed lines) based on a radiosonde observation (Meiningen) for case 1 (black) and from GDAS (grid point Leipzig) for case 2 (red).

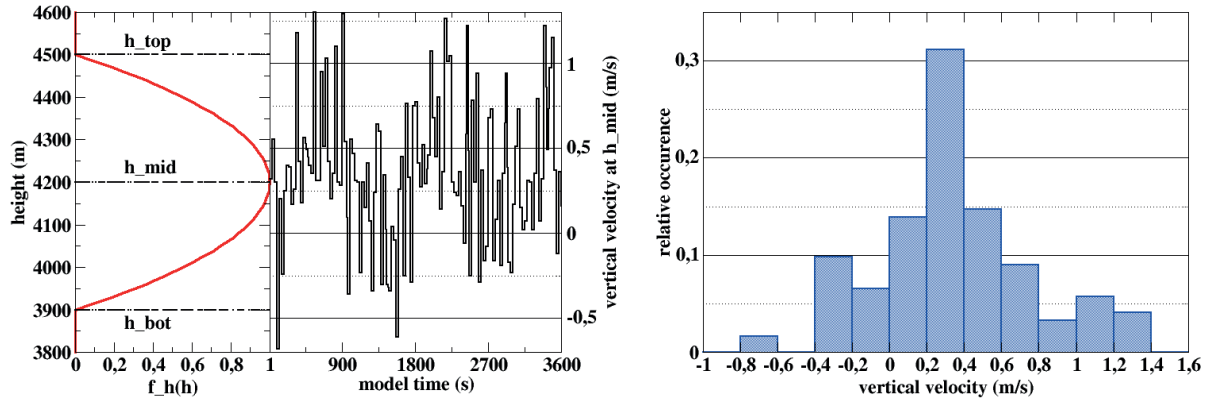


Fig. 8. Vertical velocity field of the inner cylinder for case 1. Left: Height dependence (red line) and temporal evolution of one realization of the stochastic vertical velocity field (black line) for $w_{ave} = 0.3$ m/s at h_{mid} . Right: Histogram of velocity field. Vertical velocity for case 2 is identical but for heights between 7100 m and 7700 m.

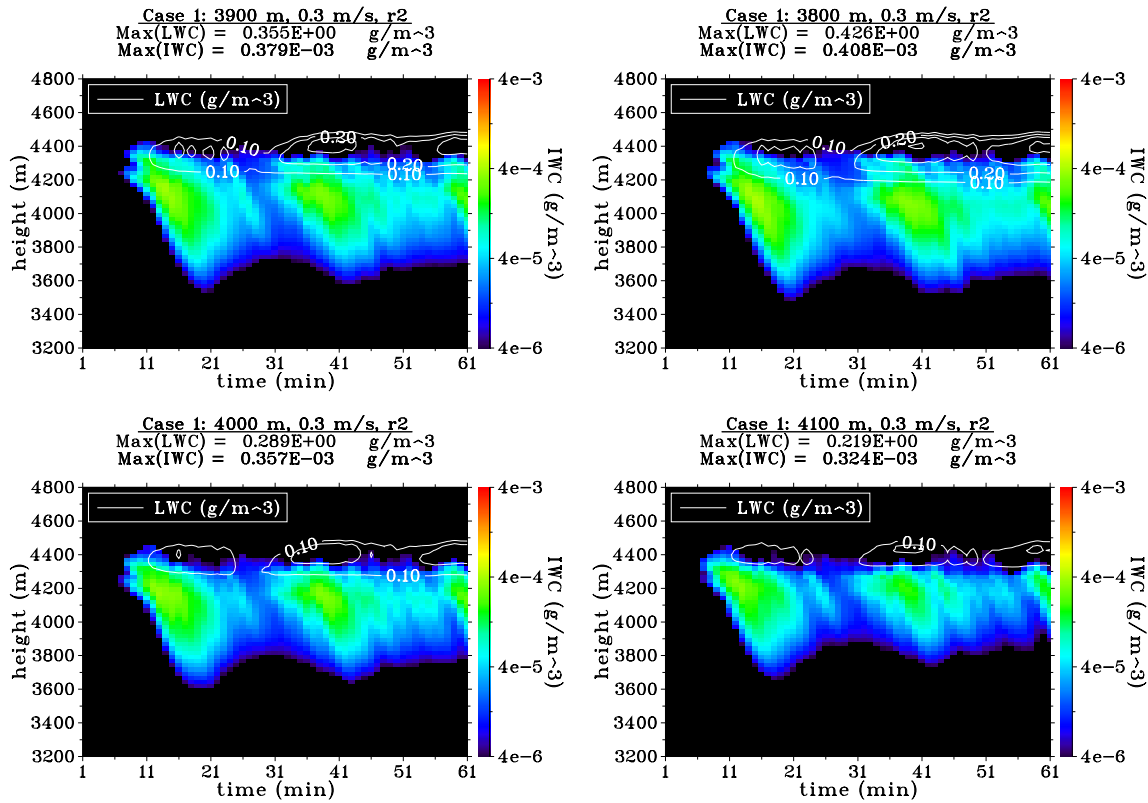


Fig. 9. Liquid LWC (contours) and ice-water-mixing-ratio IWC (colours, logarithmic scale) for case 1. Comparison of different values for h_{bot} (Upper left: W_{base} , $h_{bot} = 3900$ m, upper right: W_{h38} , $h_{bot} = 3800$ m, lower left: W_{h40} , $h_{bot} = 4000$ m, lower right: W_{h41} , $h_{bot} = 4100$ m.)

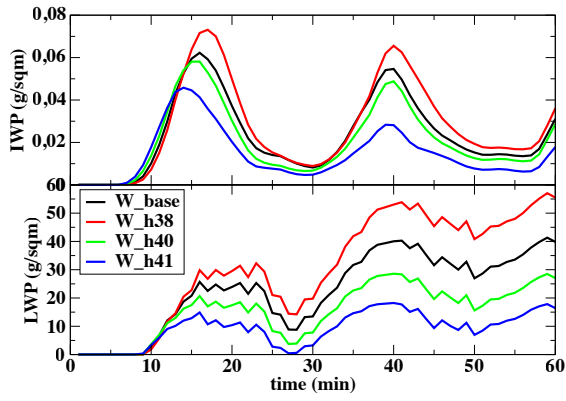


Fig. 10. Liquid (lower panel) and ice water paths (upper panel) for case 1. Comparison of the different values for h_{bot} .

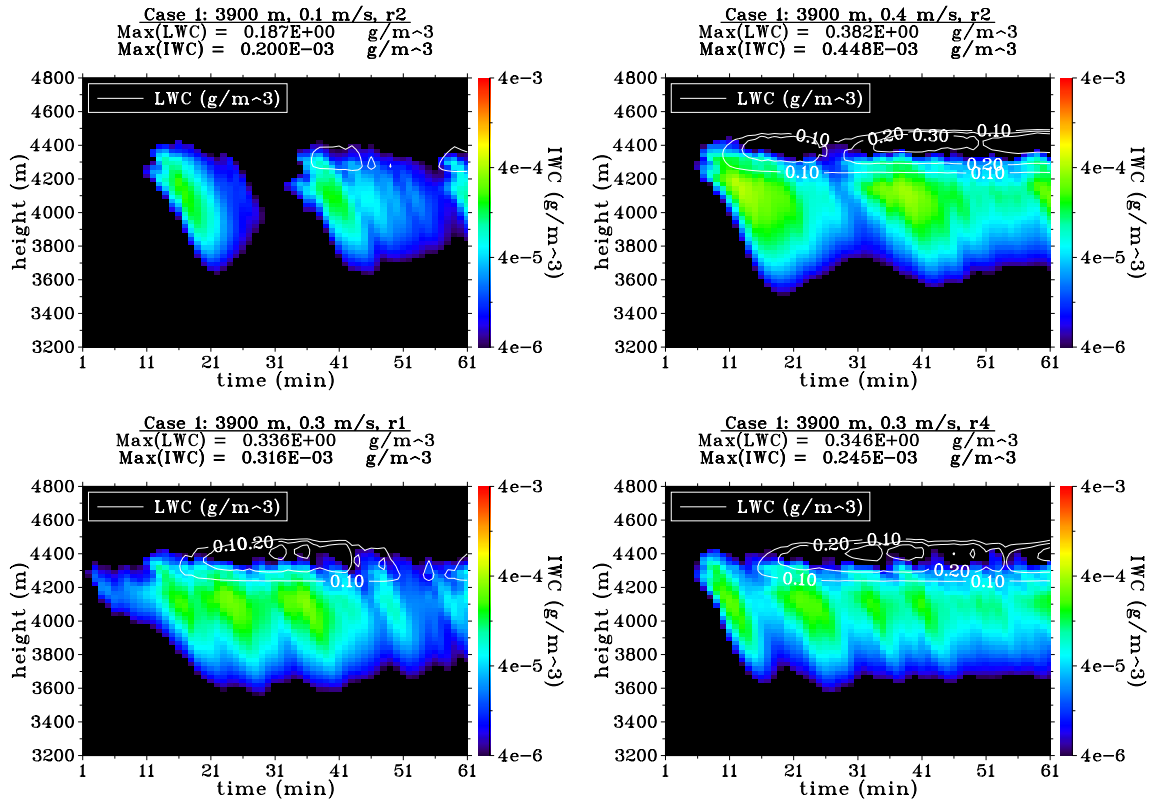


Fig. 11. Liquid LWC (contours) and ice water mixing ratio IWC (colours, logarithmic scale) for case 1. Comparison of different average updraft velocities w_{ave} (Upper panel: Left: W_w01, $w_{ave} = 0.1$ m/s, right: W_w04, $w_{ave} = 0.4$ m/s.) and different stochastic realizations (Lower: Left: W_r1, r1, right: W_r4, r4).

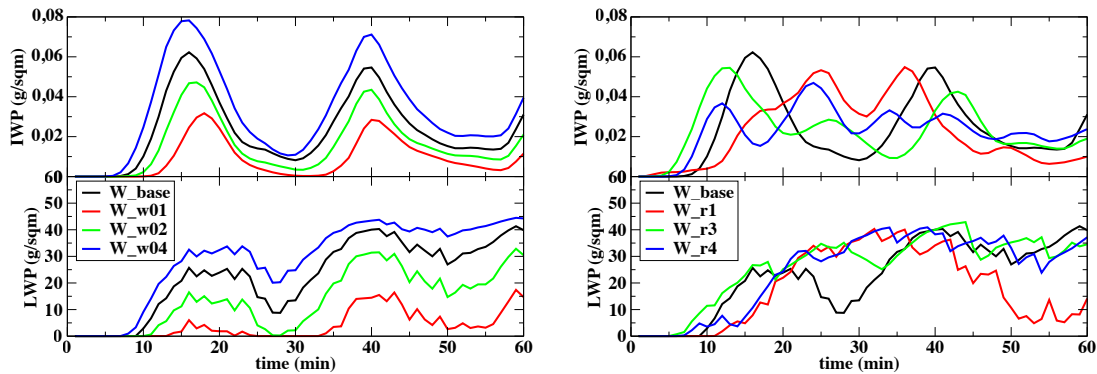


Fig. 12. Liquid (lower panels) and ice water paths (upper panels) for case 1. Comparison of the different values for w_{ave} (left) and the different stochastic realizations (right).

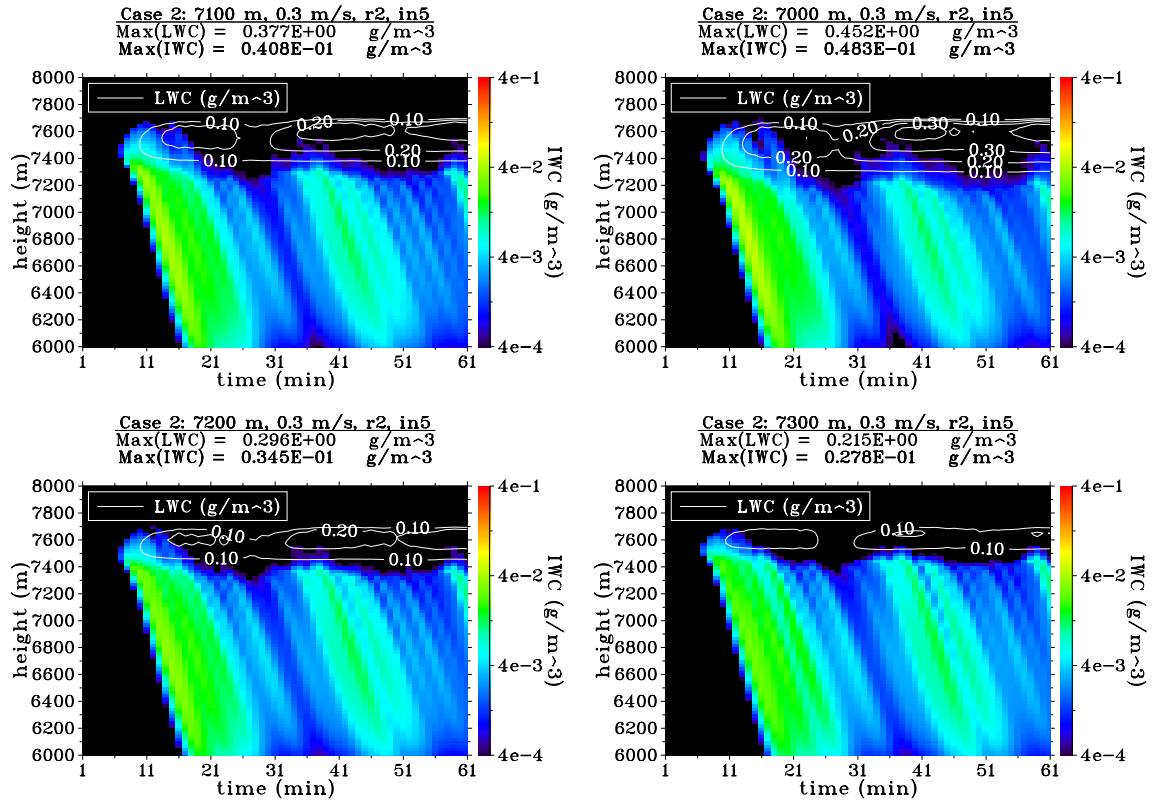


Fig. 13. Liquid LWC (contours) and ice-water-mixing-ratio IWC (colours, logarithmic scale) for case 2. Comparison of different values for h_{bot} (Upper left: C.base, $h_{bot} = 7100$ m, upper right: C.h70, $h_{bot} = 7000$ m, lower left: C.h72, $h_{bot} = 7200$ m, lower right: C.h73, $h_{bot} = 7300$ m.)

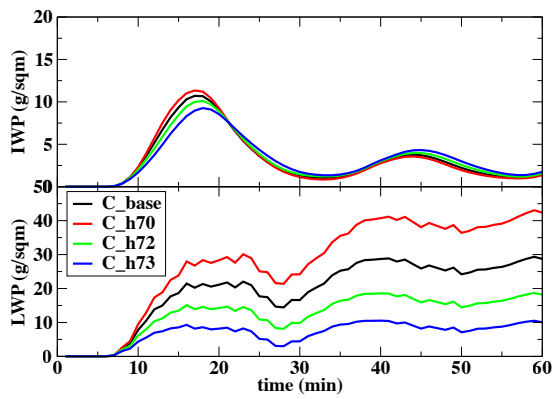


Fig. 14. Liquid (lower panel) and ice water paths (upper panel) for case 2. Comparison of the different values for h_{bot} .

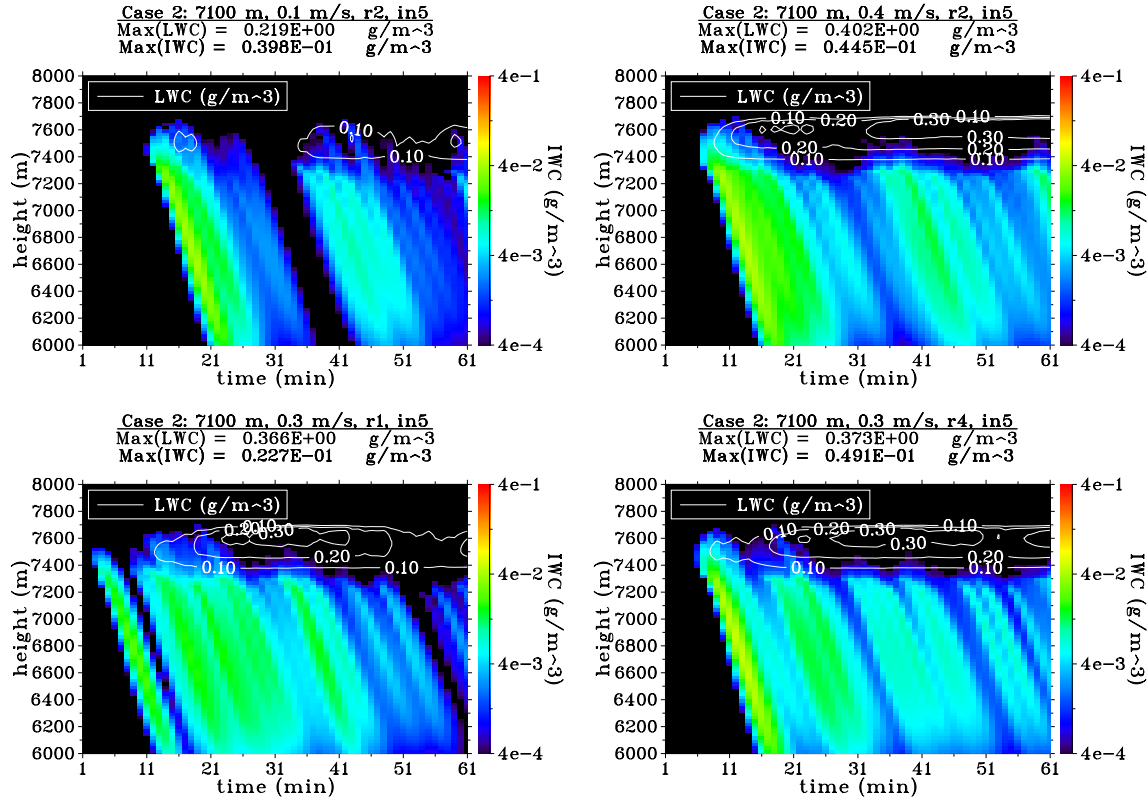


Fig. 15. Liquid LWC (contours) and ice-water mixing ratio IWC (colours, logarithmic scale) for case 2. Comparison of different average updraft velocities w_{ave} (Upper: Left: C_w01, $w_{ave} = 0.1$ m/s, right: C_w04, $w_{ave} = 0.4$ m/s) and the different stochastic realizations (Lower: Left: C_r1, r1, right: C_r4, r4).

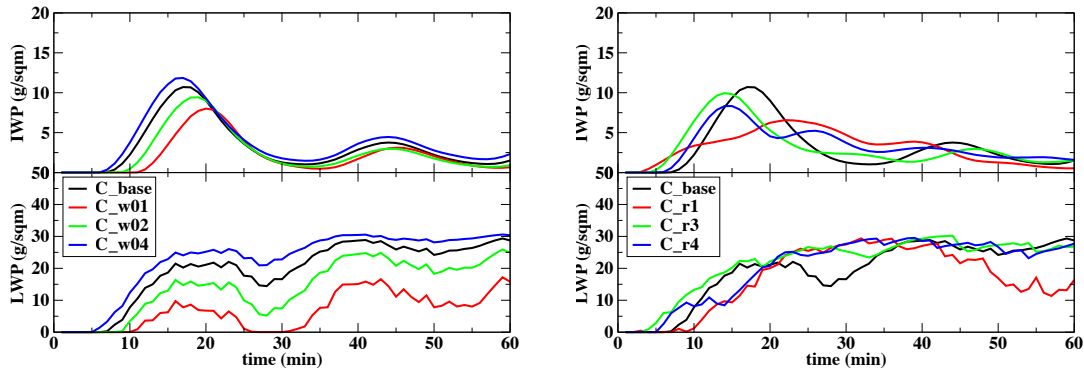


Fig. 16. Liquid (lower panels) and ice water paths (upper panels) for case 2. Comparison of the different values for w_{ave} (left) and the different stochastic realizations (right).

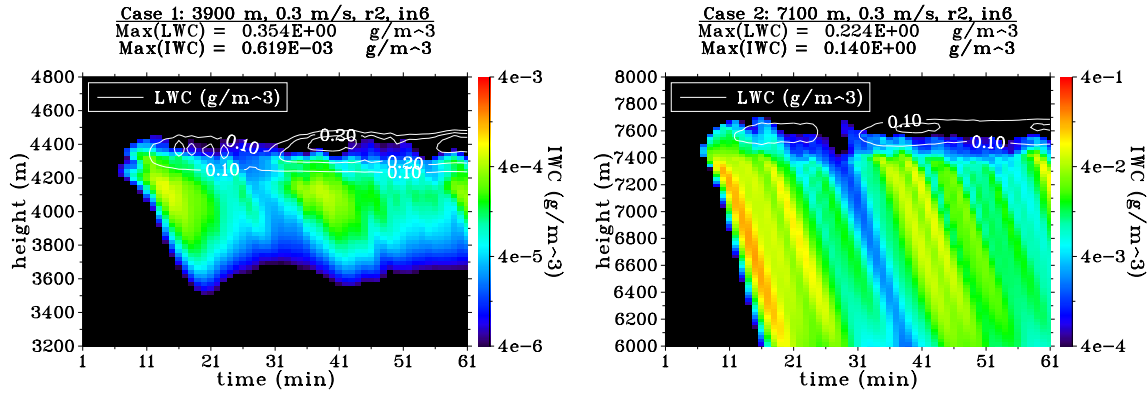


Fig. 17. Liquid-LWC (colors) and ice-water-mixing-ratio IWC (contours, logarithmic scale) for case 1 (W_in6, left) and case 2 (C_in6, right). Enhancing IN by increasing $N_{AP,r>250nm}$ by a factor of 10.

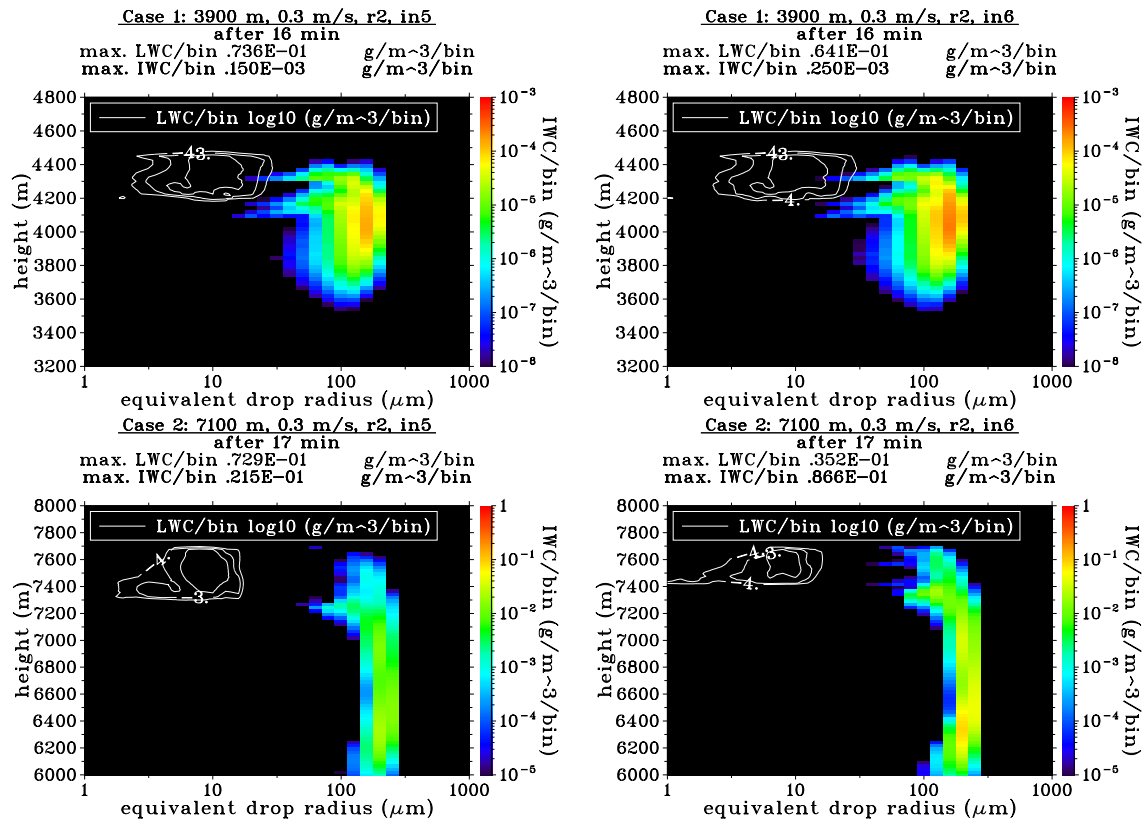


Fig. 18. Liquid-LWC (colors) and ice-water-mass-IWC per bin (contours, both logarithmic scale) for case 1 (upper panel) and case 2 (lower panel) for the respective base case (left) and the case with enhanced IN number (right; in6) after 16 and 17 minutes model time, respectively, corresponding to the IWP maximum of the base case runs.

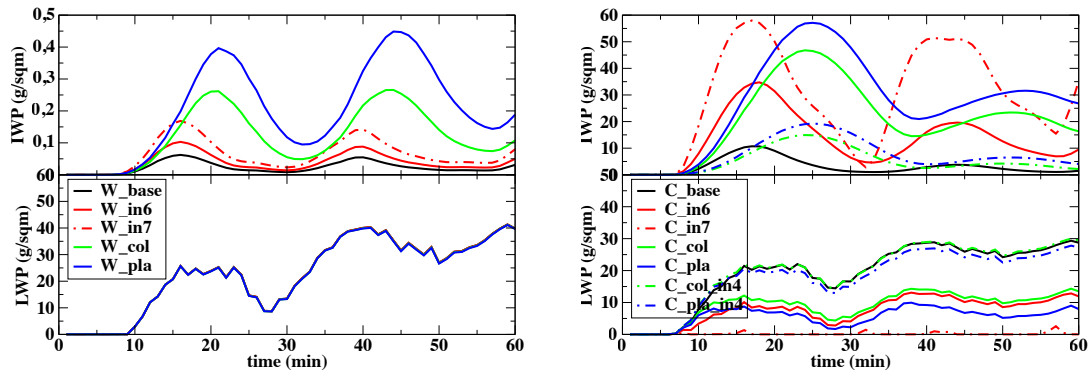


Fig. 19. Liquid (lower panel) and ice water paths (upper panel) for case 1 (left) and case 2 (right). Comparison of the sensitivities with respect to IN number and ice particle shape.

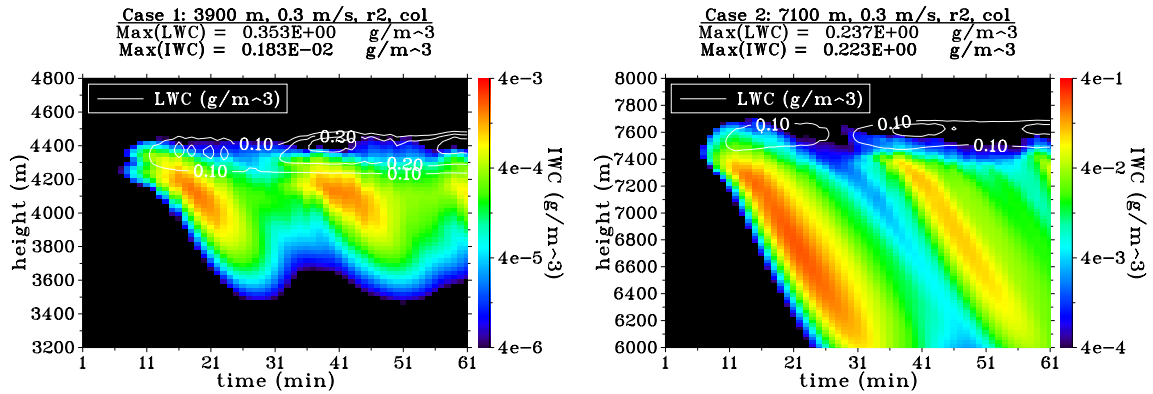


Fig. 20. Liquid LWC (color contours) and ice-water mixing ratio IWC (contour colors, logarithmic scale). Results for changing ice particle shape to hexagonal columns for case 1 (W_col, left) and case 2 (C_col, right).

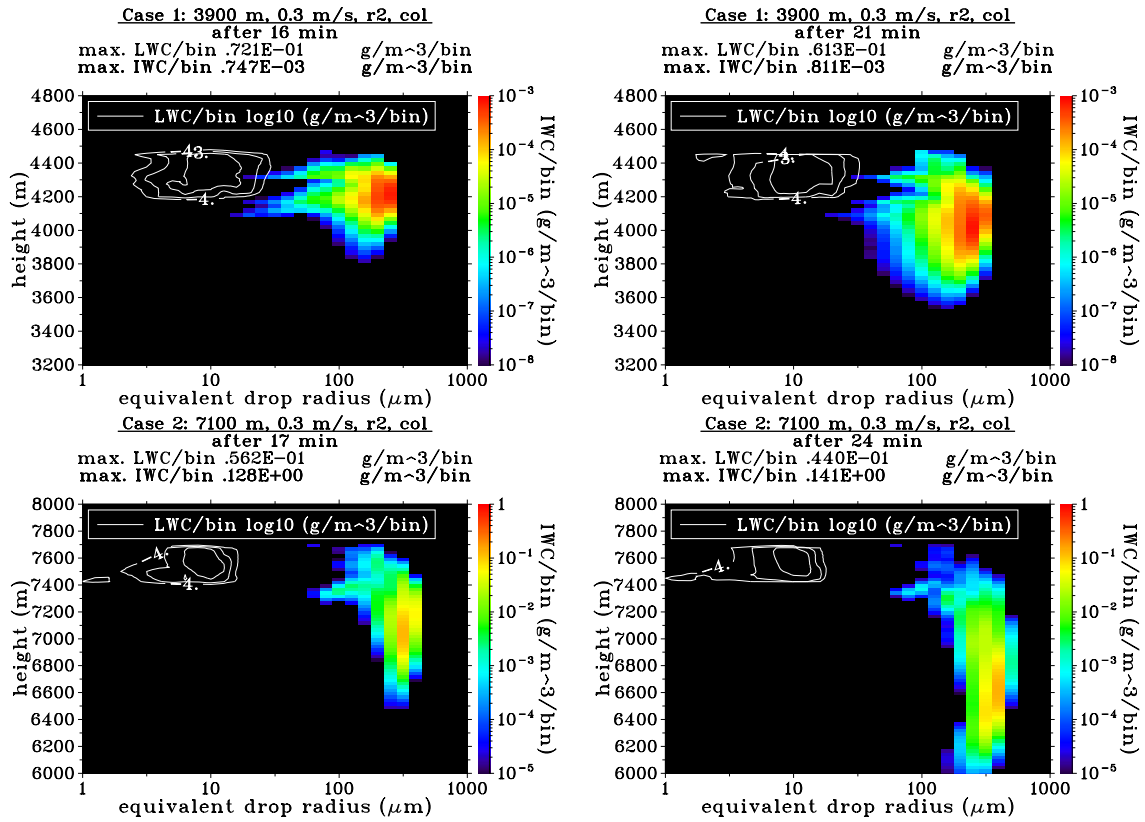


Fig. 21. Liquid-LWC (color contours) and ice water mass per bin (contours colors, both logarithmic scale) for case 1 (upper panel) and case 2 (lower panel) assuming columns as ice particle shape at IWP maximum of the respective base case (left) and at IWP of the run (right).